

## **Post-Quench Ductility Results for Zry-4 and ZIRLO Oxidized at 1000°C and 1100°C**

Y. Yan, T. Burtseva and M. Billone  
January 31, 2004

### **Summary**

Ring compression tests have been completed for Zry-4 and ZIRLO samples oxidized to nominal ECR values of 5, 10, 15, 17 and 20% at 1000°C and 1100°C. The 25-mm-long samples were exposed individually to two-sided steam oxidation in the same test apparatus for the same test times, slow cooled to 800°C and water-quenched. The test times corresponding to the nominal ECR values were calculated based on the Cathcart-Pawel (CP) weight gain correlation and a 0.57-mm-thick wall. Based on sample weight increase (normalized to the surface area), weight gain was determined and compared to CP predictions. As expected, good agreement was achieved among both alloys and the predictions for the 1100°C samples, while some differences in weight gain vs. time were observed for the 1000°C samples at the higher test times. For the highest oxidation time ( $\approx 3400$  s) at 1000°C, the ZIRLO weight gain was  $\approx 20\%$  less than that for Zry-4. These experimental weight gains, along with the sample thickness, were used to determine experimental ECR values.

Ring-compression samples (8-mm-long) were cut from the oxidized samples and tested in a Model 4505 Instron at room temperature and 2 mm/min. cross-head displacement rate. This rate corresponds to a diametral strain rate of 0.35%/s for the 9.50-mm-OD cladding. Load-displacement curves were analyzed by the offset-displacement method to determine plastic ductility. As-received (non-oxidized) samples were tested to verify that the effective stiffness for the load-displacement curves agrees with predictions for ring stiffness ( $\approx 1$  kN/mm). It was also found that the permanent displacement of non-oxidized rings compressed to 2 mm was  $\approx 1$  mm based on direct post-test measurement and  $\approx 1.2$  mm based on the offset method. Because the offset method gives values  $\approx 0.2$ -mm greater than the measured permanent strain, samples with  $\leq 0.2$  mm ( $\approx 2\%$ ) offset displacement are considered to be brittle. Both alloys exhibited offset strains  $> 2\%$  and were assessed as ductile. The 1000°C results were interesting in that ZIRLO and Zry-4 retained  $\approx 3\%$  ductility after oxidation for the same test time ( $\approx 3400$  s), even though the measured ECR values were 22.4% for Zry-4 and 18.0% for ZIRLO. These results suggest that embrittlement may correlate better with oxidation time at 1000°C and CP-predicted ECR than with measured weight gain and measured ECR.

Metallographic, microhardness and hydrogen-content analyses were performed on the highest ECR samples. These data, along with physical examination of the compressed samples, proved very useful in supporting post-quench-ductility evaluation.

## 1. Introduction

The purpose of this program is to determine the post-quench ductility of advanced cladding alloys ZIRLO and M5, as compared to the post-quench ductility of Zry-4. While extensive literature data are available for traditional Zircaloy claddings (Zry-4 and Zry-2), relatively little data have been published for ZIRLO and M5. Also, the published data for advanced alloys were generated in different laboratories by very different methods. In this program, all samples are oxidized in the same apparatus at the same ramp rates, hold times, and cooling rates (slow-cooled to 800°C and water-quenched). The 25-mm-long samples are exposed to two-sided steam oxidation prior to cooling. Also, the samples are compressed in the same Instron machine, and the load-displacement data are analyzed by a common method to determine ductility.

The Zry-4 and ZIRLO tubing (17×17 PWR) provided by Westinghouse has an outer diameter of 9.50 mm and a wall thickness of 0.57 mm. The M5 tubing (17×17 PWR) provided by Framatome has an outer diameter of 9.50 mm and a wall thickness of 0.61 mm. Table 1 summarizes the test matrix for oxidizing the samples prior to ring-compression, post-quench ductility testing. The times listed are the equivalent isothermal times at the test temperature to give Cathcart-Pawel (CP) calculated ECR values of 5, 10, 15, 17, and 20%, for an assumed wall thickness of 0.57 mm. Actual ECR values vary depending on the weight gain for each sample and the as-fabricated thickness of the sample.

Following oxidation and quench, 8-mm rings were cut from near the middle of the 25-mm-long samples. Ring compression tests were performed at room temperature at a displacement rate of 2 mm/min. The load-displacement curves were analyzed by the traditional offset-displacement method. The offset displacement, which is a measure of permanent displacement, was normalized to the outer diameter (9.50 mm) to give a nominal plastic hoop strain. Samples that exhibited offset strains >2% were considered to be ductile. To aid in the interpretation of the load-displacement curves, post-test samples were examined physically, additional limited-displacement tests were conducted, and selective characterization (metallography, microhardness, and hydrogen analysis) was performed.

## 2. Steam Oxidation and Quench

References 1 (M5 and Zry-4) and 2 (ZIRLO and Zry-4) describe the apparatus used to oxidize and quench the samples, along with thermal, chemical and metallographic verification and validation test results. Tables 2 and 3 show the measured weight gain and ECR values vs. predicted ECR values for the 1000°C and 1100°C oxidation temperatures, respectively. Figures 1-2 show, respectively, the weight gain results for ZIRLO and Zry-4 at 1000°C and 1100°C. The 1100°C results indicate that weight gain kinetics for both alloys are comparable and in agreement with the Cathcart-Pawel correlation. The 1000°C weight-gain results indicate that ZIRLO < Zry-4 for test times greater than ≈1000 s.

Table 1 Test Matrix for Oxidation of Samples for Post-Quench Ductility Tests. The times and ECR values listed correspond to those calculated using the Cathcart-Pawel weight gain correlation, a nominal wall thickness of 0.57 mm, and two-sided isothermal oxidation in steam. The relationship between ECR (%) and normalized weight gain ( $\Delta w$  in  $\text{mg}/\text{cm}^2$ ) is  $\text{ECR} = 1.538 \Delta w$  for 0.57-mm-thick cladding samples.

<b>Temperature °C</b>	<b>ECR %</b>	<b>Equivalent Oxidation Time s</b>
1000	5	210
	10	841
	15	1892
	17	2430
	20	3364
1100	5	67
	10	266
	15	599
	17	769
	20	1065
1200	5	25
	10	99
	15	222
	17	285
	20	394
1260	5	14
	10	58
	15	130
	17	167
	20	231

Table 2 Weight Gain ( $\Delta w$  in  $\text{mg}/\text{cm}^2$ ) and Measured ECR (%) Values for Zry-4 and ZIRLO Oxidized in Steam at  $1000^\circ\text{C}$ .  $\text{ECR} = 1.538 \Delta w$  for the 0.57-mm wall thickness. Alloys were oxidized for the same ramp rate, hold time and cooldown rate for each nominal ECR value.

Cathcart-Pawel ECR, %	Material	Measured Weight Gain ( $\Delta w$ ), $\text{mg}/\text{cm}^2$	Measured ECR, %
5	Zry-4 ZIRLO	3.9 3.8	6.1 5.9
10	Zry-4 ZIRLO	7.2 6.8	11.0 10.5
15	Zry-4 ZIRLO	11.0 9.0	16.9 13.8
17	Zry-4 ZIRLO	12.5 10.8	19.3 16.6
20	Zry-4 ZIRLO	14.6 11.7	22.4 18.0

Table 3 Weight Gain ( $\Delta w$  in  $\text{mg}/\text{cm}^2$ ) and Measured ECR (%) Values for Zry-4 and ZIRLO Oxidized in Steam at  $1100^\circ\text{C}$ .  $\text{ECR} = 1.538 \Delta w$  for the 0.57-mm wall thickness. Alloys were oxidized for the same ramp rate, hold time and cooldown rate for each nominal ECR value.

Cathcart-Pawel ECR, %	Material	Measured Weight Gain ( $\Delta w$ ), $\text{mg}/\text{cm}^2$	Measured ECR, %
5	Zry-4 ZIRLO	4.0 3.8	6.2 5.9
10	Zry-4 ZIRLO	7.1 7.1	10.9 10.9
15	Zry-4 ZIRLO	10.6 10.5	16.3 16.1
17	Zry-4 ZIRLO	11.7 11.6	18.0 17.9
20	Zry-4 ZIRLO	13.2 13.7	20.3 21.1

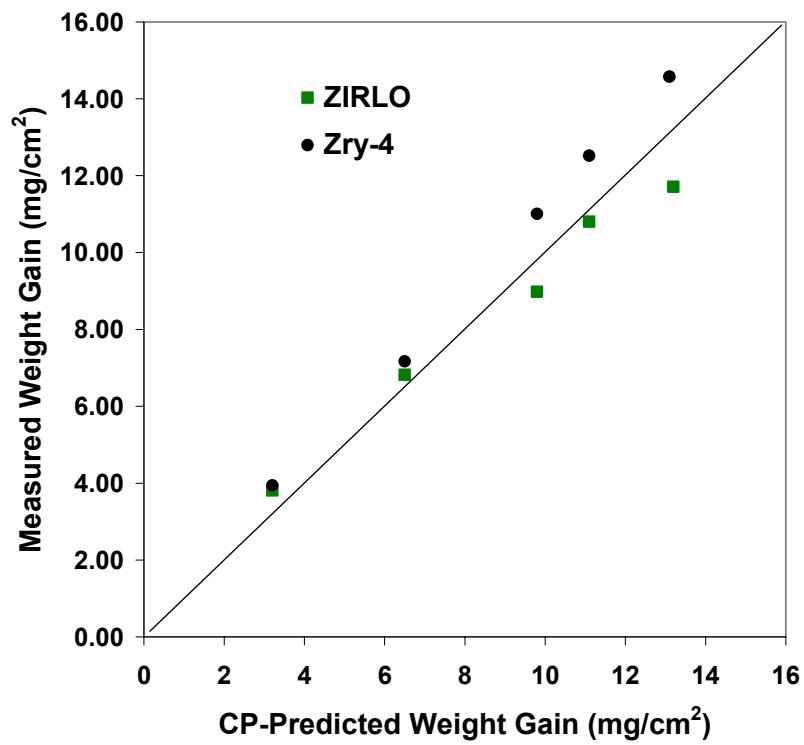


Fig. 1. Comparison between weight gain data for ZIRLO and Zry-4 and weight gain predicted by the Cathcart-Pawel (CP) correlation for samples oxidized (two-sided) in steam at 1000°C. Test times correspond to CP-calculated ECR values of 5, 10, 15, 17, and 20%.

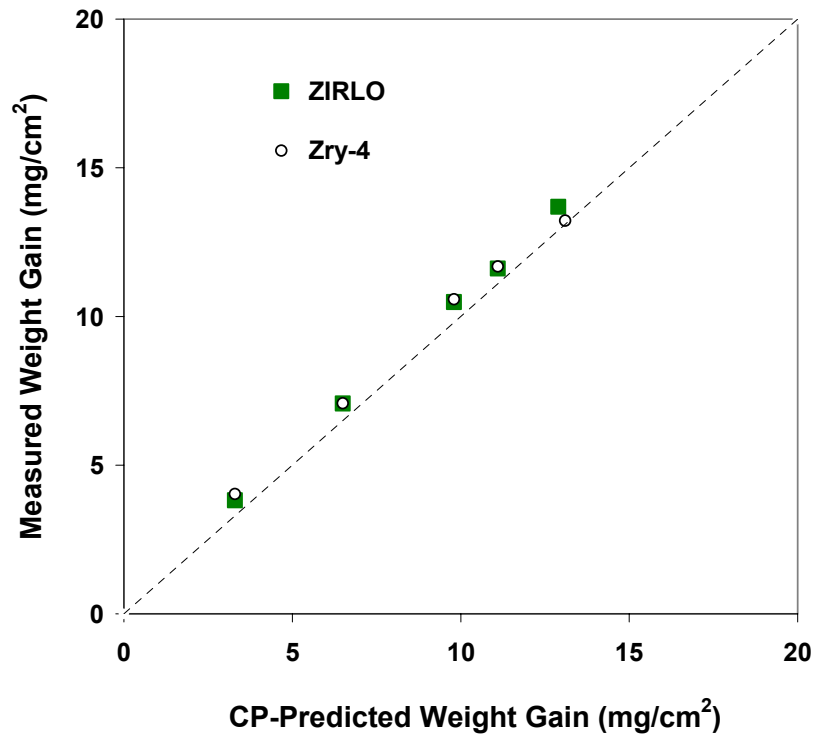


Fig. 2. Comparison between weight gain data for ZIRLO and Zry-4 and weight gain predicted by the Cathcart-Pawel (CP) correlation for samples oxidized (two-sided) in steam at 1100°C. Test times correspond to CP-calculated ECR values of 5, 10, 15, 17, and 20%.

### 3. Ring Compression Tests

#### 3.1 Validation of Ring Compression Test and Data-Analysis Methodology

Ring compression tests were conducted at room temperature on 8-mm-long samples prepared from the central region of the 25-mm-long oxidized-and-quenched samples. Flat support and loading machine fixtures were used to compress the rings. Tests were conducted at a cross-head displacement rate of 2 mm/min. Normalizing this to the outer-diameter (9.50 mm) of the tubing gives a diametral strain rate of 0.35%/s. A Model 5566 table-top Instron machine had been ordered to conduct these tests. However, as there was a delay in delivery of this new Instron, the Model 4505 Instron, belonging to the ET Ceramics Section, was used. Initial tests were conducted on as-received tubing to compare the predicted ring elastic stiffness to the linearized slope of the load-displacement curve. The load-displacement curves gave an effective elastic stiffness of  $\approx 1$  kN/mm, which is in good agreement with the predicted value. Thus the machine stiffness is large relative to the sample stiffness. Additional ring-compression tests were conducted on validation samples of Zry-4, ZIRLO and M5, which had been oxidized and slow cooled without quench. A few validation samples, which had been subjected to quench, were also tested. “Ductility” was determined by the offset-displacement method used for interpretation of load-displacement curves for metals. Figure 3 shows the load-displacement curve for a ZIRLO validation sample oxidized to 18% ECR at 1100°C and cooled without quench. The first significant load drop indicates the first through-wall failure. The offset displacement method is illustrated on this curve. The method assumes that if the sample were unloaded just prior to cracking, it would unload with the same stiffness as the linearized portion of the initial load rise. This gives an offset displacement of 0.203 mm for the Fig. 3 sample. Dividing by the outer diameter (9.50 mm) to determine a nominal plastic hoop strain gives  $\approx 2\%$  offset strain. A similar validation test was performed with a Zry-4 sample oxidized to 18% ECR and cooled without quench. The sample exhibited an offset strain of  $\approx 4\%$ , which implies ductile behavior. Hydrogen analysis and metallography were performed on this Zry-4 sample to support the conclusion that the sample should behave in a ductile manner from a materials perspective. The hydrogen pickup was low (8 wppm), indicating no hydrogen embrittlement. Also, the low-oxygen-containing prior-beta layer, which is ductile, was effectively thick enough to support the ductile behavior determined from the offset-displacement method.

In addition to the ring-compression validation tests with oxidized Zry-4 and ZIRLO, numerous tests were conducted with E110 cladding samples oxidized at 1100°C (one-sided) and 1000°C (two-sided) [3]. As this cladding embrittles at relatively low ECR values due to early breakaway oxidation and hydrogen pickup  $>200$  wppm, the results were used to validate the determination of the ductile-to-brittle transition by means of the ring compression test offset strain. These ring compression results are documented in a separate report for the E110 samples oxidized at 1000°C [4].



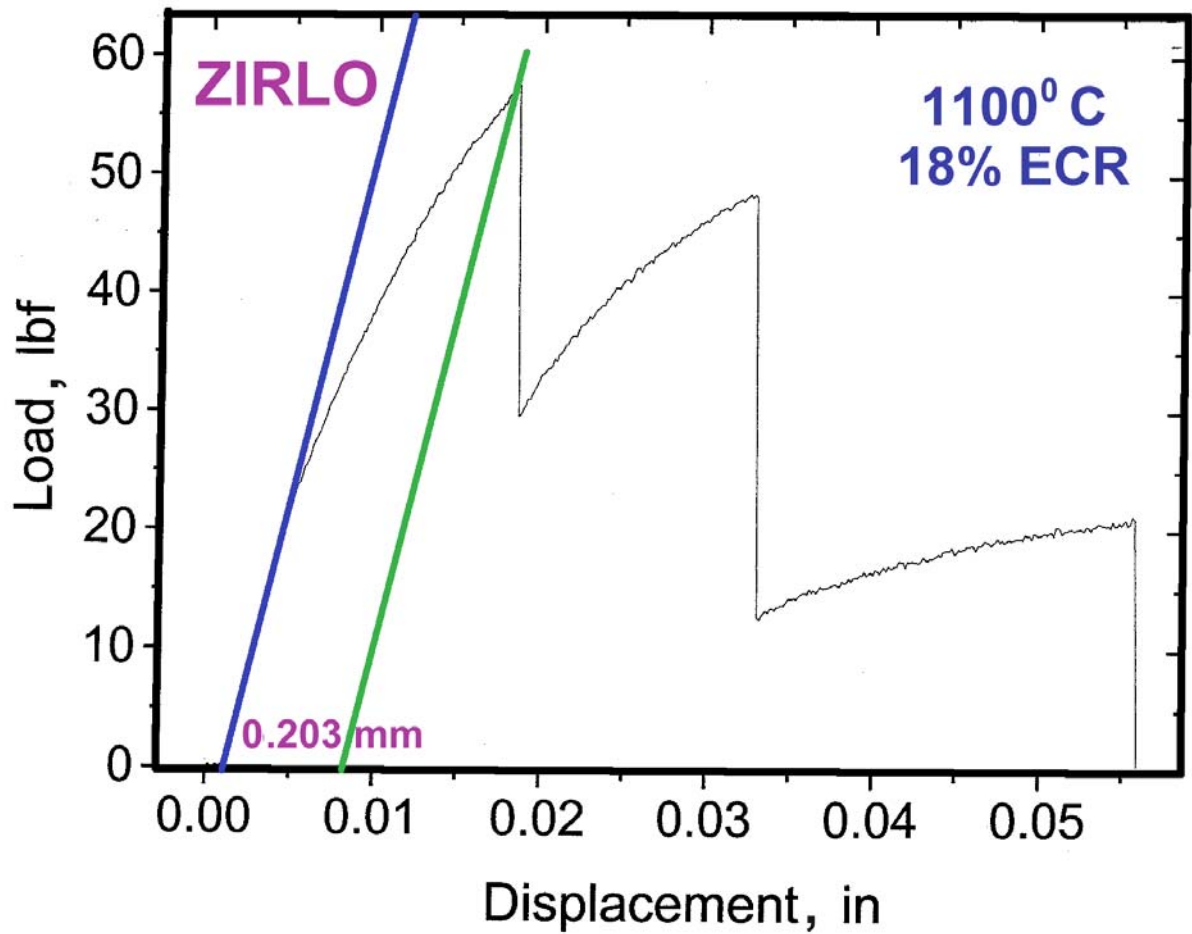


Fig. 3. Load-displacement curve for validation ZIRLO sample oxidized at 1100°C to 18% ECR without quench. Ring compression test was conducted at room temperature and a cross-head displacement rate of 2 mm/minute. The offset displacement is 0.203 mm. Normalizing this displacement to the tubing diameter (9.5 mm), gives a nominal plastic ductility of 2.1% in the hoop direction.

### 3.2 Post-Quench, Ring-Compression Data

From the samples listed in Tables 2 and 3, 8-mm-long rings were cut from the central region for ring-compression testing. As with the validation tests, these tests were conducted at room temperature and a cross-head displacement rate of 2 mm/min. The load-displacement curves from these tests are given in Appendix A for Zry-4 and in Appendix B for ZIRLO. Determination of offset displacement and strain for the 1000°C and 1100°C samples with the highest ECR values proved to be relatively straightforward. These samples exhibited four distinct load drops and broke into 4 pieces. The first significant load drop, which indicates through-wall failure, is very abrupt and occurs at relatively low displacement. However, at intermediate ECR values, it was often difficult to determine the load drop or decrease indicating failure. Cracking of the very brittle, high-oxygen alpha layers, as well as the brittle oxide layers, generates load drops that do not necessarily indicate through-wall failure. In order to interpret the load-displacement curves to determine offset strain, it was necessary to examine the intermediate-ECR samples to determine if indeed a through-wall crack was present. The observations are included in the figure captions in the Appendices.

In addition to physical inspection of the samples, a number of additional ring-compression tests were conducted with the new Instron (Model 5566). As-received samples (Zry-4, ZIRLO, M5 and E110) were compressed to determine elastic stiffness from the load-displacement data as compared to the predicted ring stiffness ( $K = F/d = [E w t^3]/[1.8 R^3]$ , where  $E$  is Young's modulus,  $w$  is the width or length of the ring,  $t$  is the ring thickness, and  $R$  is the mean radius of the ring). For the as-received samples, measured  $K$  values for Zry-4 and ZIRLO were, on the average, 0.88 kN/mm compared to a predicted value of 0.86 kN/mm. Similarly, for the thicker as-received M5 samples the average (1.12 kN/mm) of the measured values was in good agreement with the predicted value (1.07 kN/mm). In addition, as-received and oxidized samples were compressed to a limited displacement. Test results for as-received samples limited to 2-mm cross-head displacement proved most interesting. For Zry-4 and ZIRLO, the offset method predicted 1.18 mm of permanent displacement, while direct post-test measurement gave 1.00 mm. For M5, the offset displacement was 0.13 mm higher than the direct post-test measurement. Because of these results, along with uncertainties regarding displacement due to partial cracking vs. plastic displacement, an offset displacement of 0.2 mm (2% nominal hoop strain) was taken as the transition strain between ductile and brittle behavior for these tests. This was then confirmed by compressing a highly oxidized sample through the first significant load drop; the offset displacement was 0.31 mm, while the post-test diameter decrease was 0.11 mm.

Tests on as-received and oxidized samples that were limited to 2 mm displacement were also interesting with regard to the evolution of deformation and failure. For very low-ductility samples, through-wall failure appears to occur first at the loading (0°) and support (180°) points, followed by failure at positions  $\pm 90^\circ$  from the load application point. For intermediate-ductility samples, the loading and support locations tend to flatten out as the material deforms, followed by cracking of the brittle layers, and either through-wall failure or buckling followed by through-wall failure. Such behavior accounts for the wide variation in the rates of load decrease observed in the load-displacement curves for intermediate ECR samples. As the flattening and buckling of the load and support portions of the ring involve relatively high bending strains, the normalization of displacement to outer diameter is not an accurate metric for high-ductility rings.

Detailed analyses of the load-displacement curves in Appendices A and C, along with post-test physical examination of the samples and displacement-limited test results, were used to determine the offset displacement and plastic hoop strain prior to through-wall failure. These are listed in Table 4 for samples oxidized at 1000°C and Table 5 for samples oxidized at 1100°C. Graphical representation of these results is shown in Figs. 4 and 5, respectively. Figures 4a and 5a show ductility vs. measured ECR, while Figs. 4b and 5b show ductility vs. the CP-predicted ECR. Based on these data, essentially all of the samples tested exhibited offset strains >2% and were classified as “ductile”.

Figure 6 and 7 show the post-test samples for Zry-4 and ZIRLO, respectively, oxidized at 1000°C (a) and 1100°C (b). The ECR values listed for identification are CP-calculated values, not measured values. (See Tables 4 and 5 for the measured values.) As some of these samples were handled and manually deformed to failure prior to photographing, refer to the figure captions in the Appendices for the actual condition of the samples prior to handling.

### 3.3 Post-test Characterization of Highest ECR Samples

Based on the data presented in Tables 4 and 5, essentially all of the samples tested are classified as “ductile” as their measured offset strains are greater than the 2% cutoff limit chosen for this study. Given that the ring compression test is really a structural test, as compared to a materials test, it is important to characterize the material to verify that it should behave in a ductile manner in the ring-compression test. From this perspective, it is essential that the hydrogen content be relatively low (<150 wppm) and that there be a sufficient amount of ductile, low-oxygen metal (prior-beta) remaining around the mid-radius of the sample. The hydrogen content is measured using the LECO Hydrogen Determinator.

Table 6 summarizes the results of the post-test characterization for Zry-4 and ZIRLO samples at the highest ECR values. At 1000°C, the hydrogen pickup for Zry-4 is low ( $\approx 20$  wppm) indicating that protective inner and outer oxide layers are still in place. The hydrogen pickup for ZIRLO at 1000°C and 18% ECR is  $\approx 100$  wppm. Although this hydrogen content is not high enough to embrittle the alloy following quench, it suggests that ZIRLO may be approaching oxide instability after  $\approx 3400$  s at 1000°C. This is supported by the measured hydrogen pickup of 33 wppm for ZIRLO at 16.6% ECR. From the arc segments in Fig. 8, it is clear that the oxide layer thicknesses follow the same trend as the weight gains: Zry-4 > ZIRLO. Also, based on the data in Table 6, it is clear that the weight-gain ratio (ZIRLO/Zry-4 = 0.80) scales with the oxide-thickness ratio (ZIRLO/Zry-4 = 0.75). It is also clear from the metallography, as well as the microhardness data, that the prior-beta layer consists of low-to-intermediate oxygen-containing metal for these alloys.

The results for the samples oxidized at 1100°C for  $\approx 1100$  s indicate low hydrogen pickup and comparable oxide layer thicknesses (see Table 6 and Fig. 9). Detailed analyses of the metallographic and microhardness results are in progress.

Table 4 Ring Compression Test Results for Samples Oxidized at 1000°C and Quenched (see Table 2). Tests were performed on 8-mm-long samples at room temperature and at 2 mm/min. cross-head displacement. A complete set of tests were performed using the Model 4505 Instron. A limited number of confirmation tests were performed with the new Model 5566 Instron on rings cut from the same 25-mm-long oxidation samples.

Cathcart-Pawel ECR, %	Material	Measured ECR %	Offset Displacement mm	Offset Hoop Strain %	Confirmation Tests Model 5566 Instron
5	Zry-4 ZIRLO	6.1 5.9	4.4 4.9	46 52	--- ---
10	Zry-4 ZIRLO	11.0 10.5	2.74 2.35	29 25	Yes Yes
15	Zry-4 ZIRLO	16.9 13.8	0.711 1.92	7.5 20	Yes Yes
17	Zry-4 ZIRLO	19.3 16.6	0.483 0.447	5.1 4.7	--- --- ---
20	Zry-4 ZIRLO	22.4 18.0	0.307 0.271	3.2 2.9	--- ---

Table 5 Ring Compression Test Results for Samples Oxidized at 1100°C and Quenched (see Table 3). Tests were performed on 8-mm-long samples at room temperature and at 2 mm/min. cross-head displacement. A complete set of tests were performed using the Model 4505 Instron. A limited number of confirmation tests were performed with the new Model 5566 Instron on rings cut from the same 25-mm-long oxidation samples.

Cathcart-Pawel ECR, %	Material	Measured ECR %	Offset Displacement mm	Offset Hoop Strain %	Confirmation Tests Model 5566 Instron
5	Zry-4 ZIRLO	6.2 5.9	5.5 5.0	58 52	--- ---
10	Zry-4 ZIRLO	10.9 10.9	1.9 2.1	20 22	--- ---
15	Zry-4 ZIRLO	16.3 16.1	0.516 0.483	5.4 5.1	--- Yes
17	Zry-4 ZIRLO	18.0 17.9	0.38 - 0.56 0.330	4 - 6 3.5	--- ---
20	Zry-4 ZIRLO	20.3 21.1	0.455 0.318	4.8 3.3	--- ---

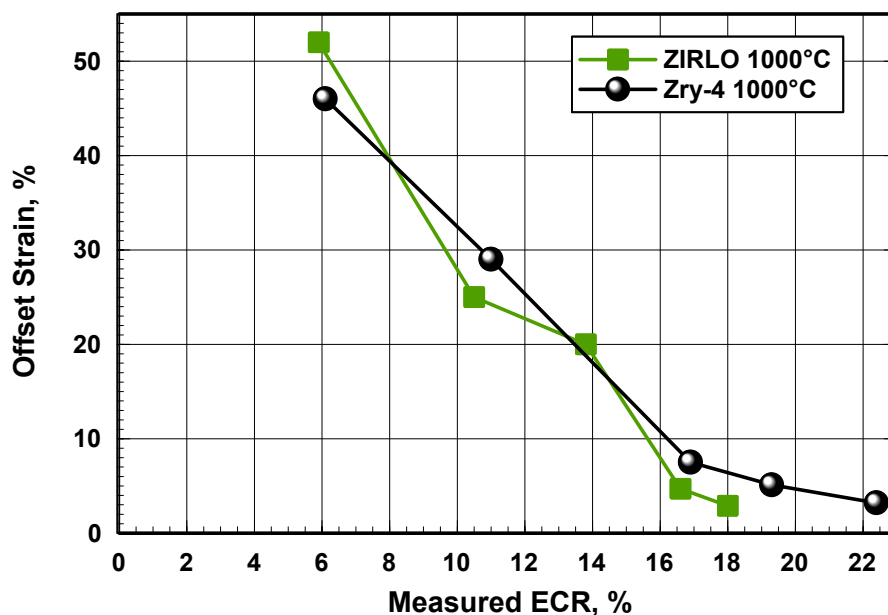


Fig. 4a. Post-quench ductility vs. measured ECR for ZIRLO and Zry-4 oxidized in steam at 1000°C. Ductility is based on offset strain determined from ring-compression tests conducted at room temperature and 2 mm/min. cross-head displacement rate.

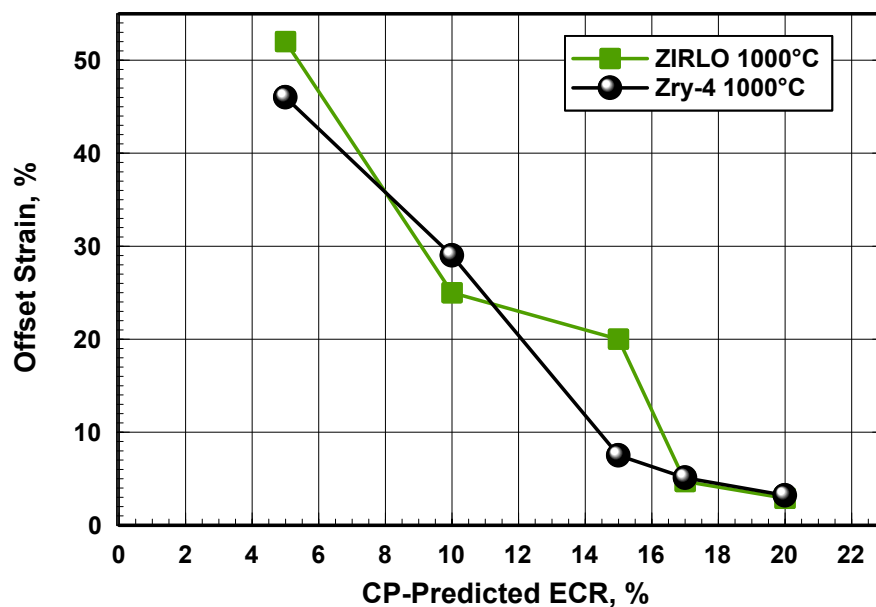


Fig. 4b. Post-quench ductility vs. CP-predicted ECR for ZIRLO and Zry-4 oxidized in steam at 1000°C. Ductility is based on offset strain determined from ring-compression tests conducted at room temperature and 2 mm/min. cross-head displacement rate.

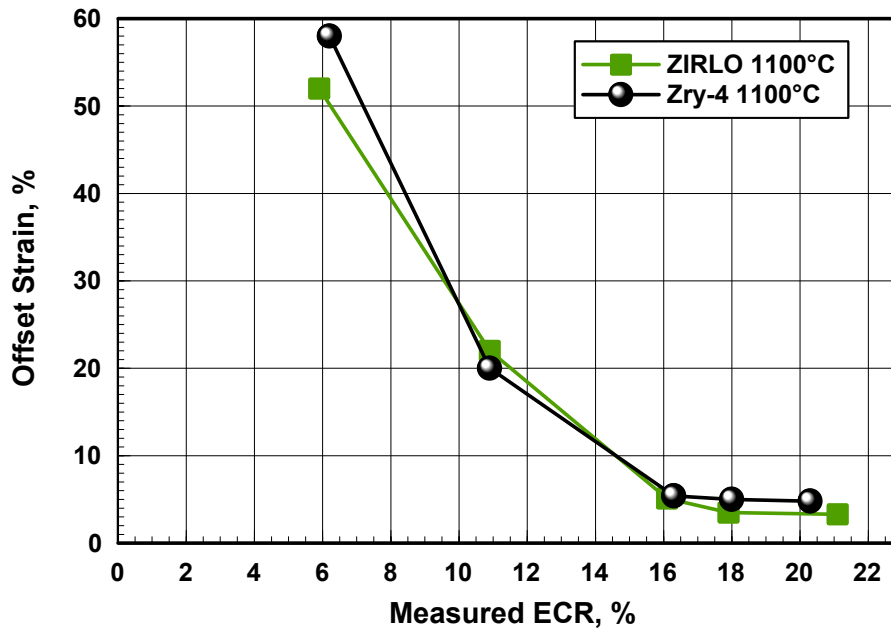


Fig. 5a. Post-quench ductility vs. measured ECR for ZIRLO and Zry-4 oxidized in steam at 1100°C. Ductility is based on offset strain determined from ring-compression tests conducted at room temperature and 2 mm/min. cross-head displacement rate.

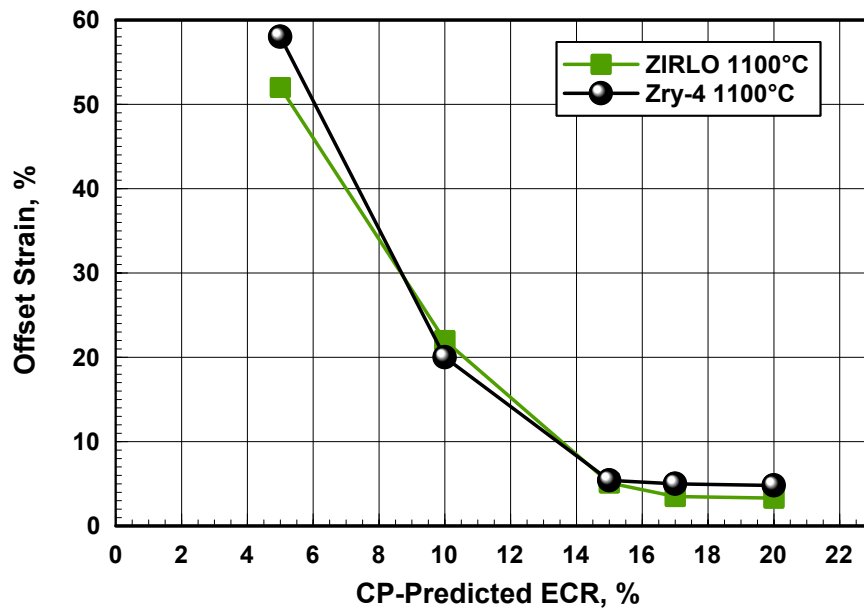
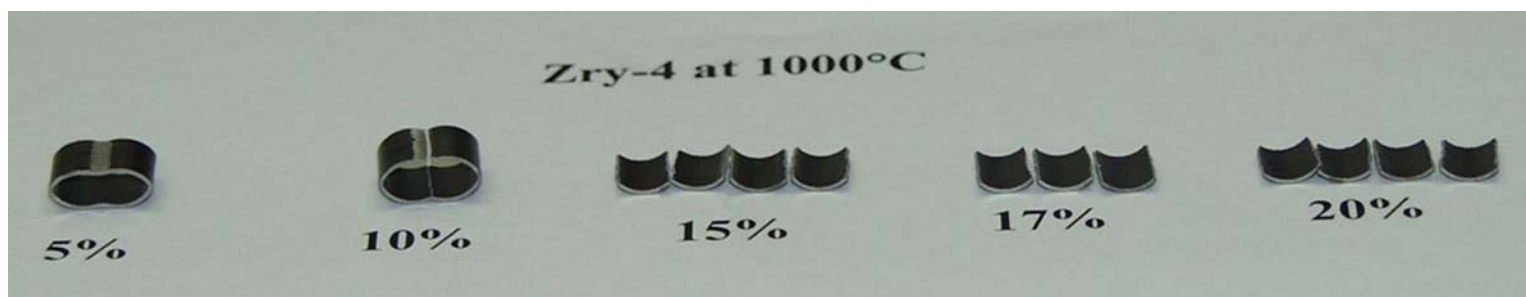
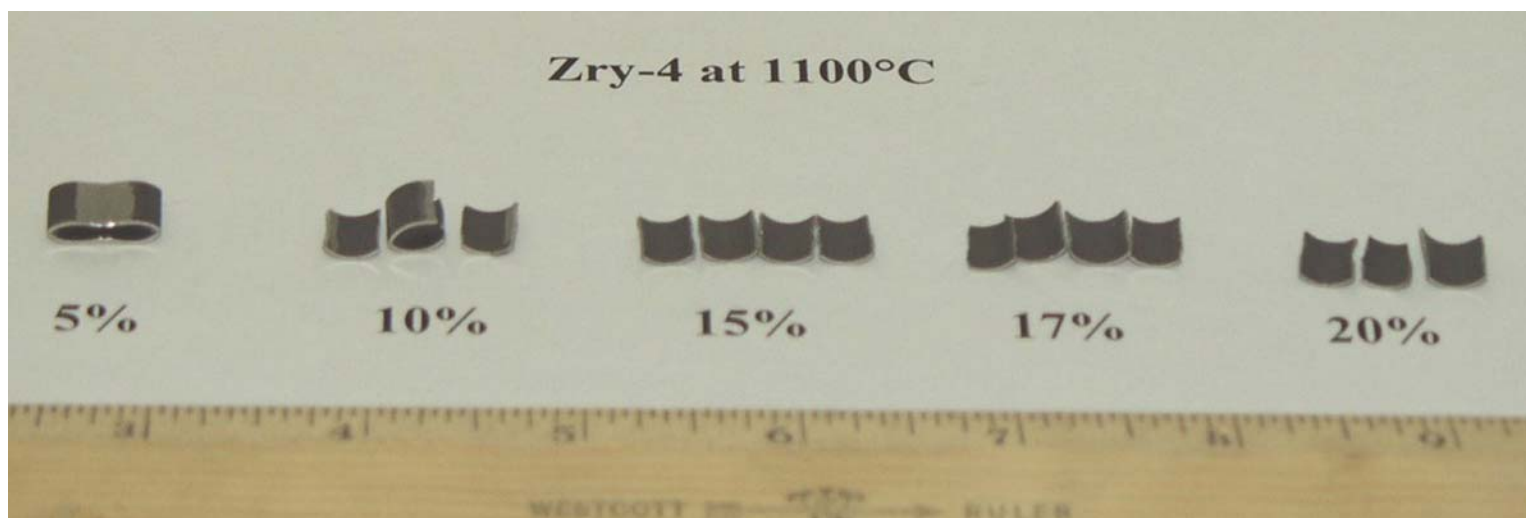


Fig. 5b. Post-quench ductility vs. CP-predicted ECR for ZIRLO and Zry-4 oxidized in steam at 1100°C. Ductility is based on offset strain determined from ring-compression tests conducted at room temperature and 2 mm/min. cross-head displacement rate.



(a)



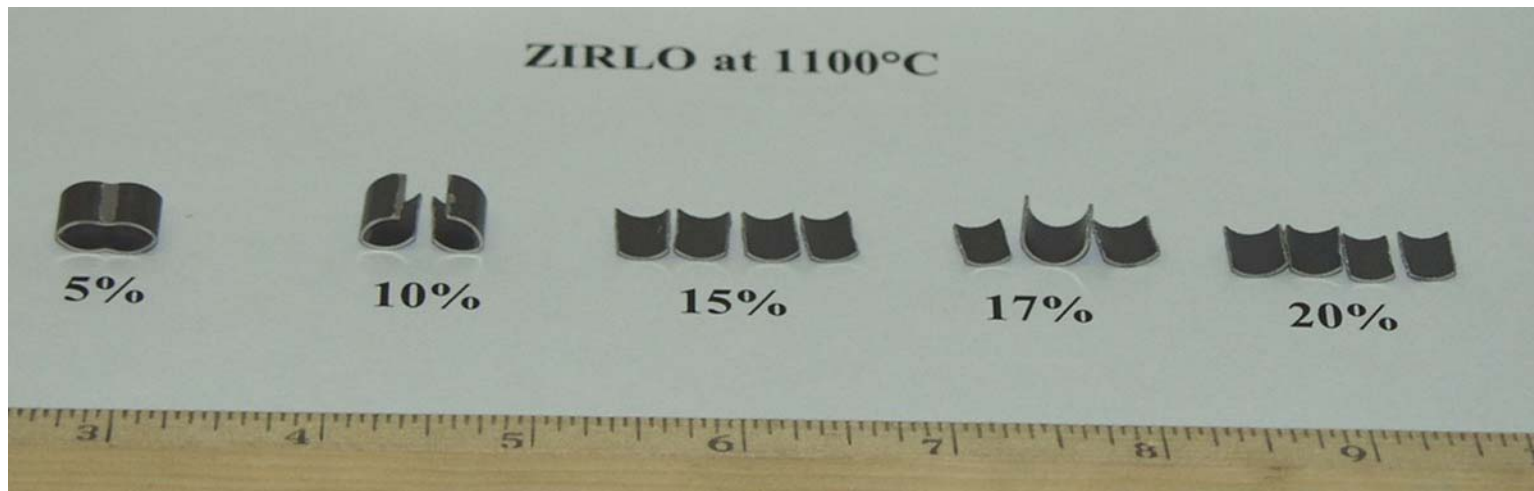
(b)

Fig. 6. Post-test appearance of Zry-4 ring-compression samples tested at room temperature and 2 mm/min: (a) samples oxidized at 1000°C; and (b) samples oxidized at 1100°C. ECR values are calculated using the Cathcart-Pawel weight gain correlation.





(a)

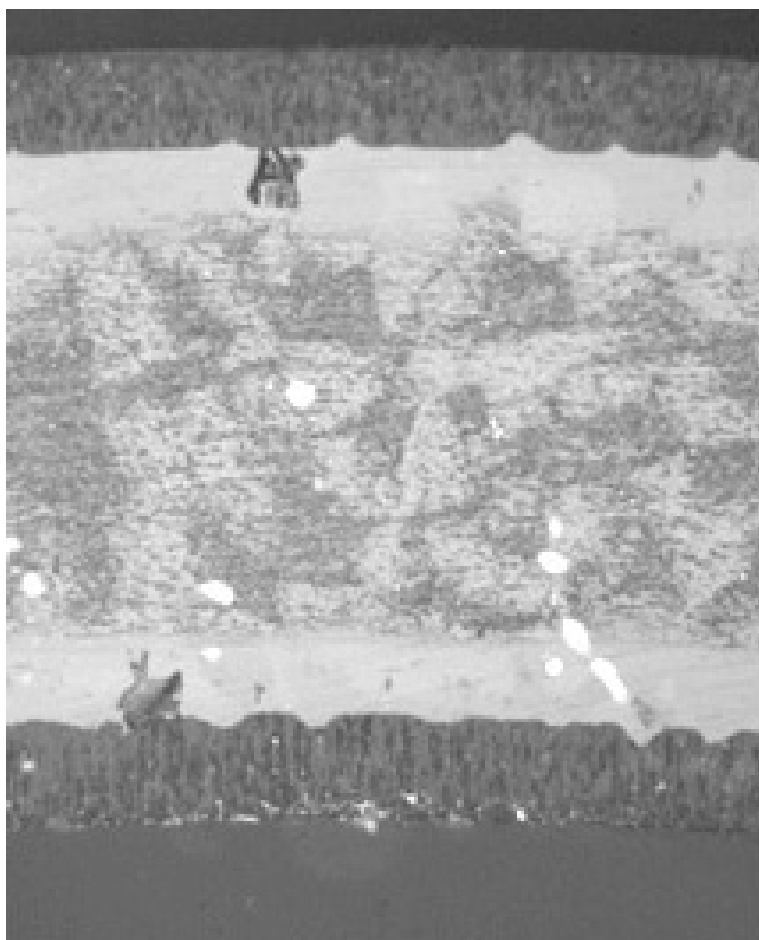


(b)

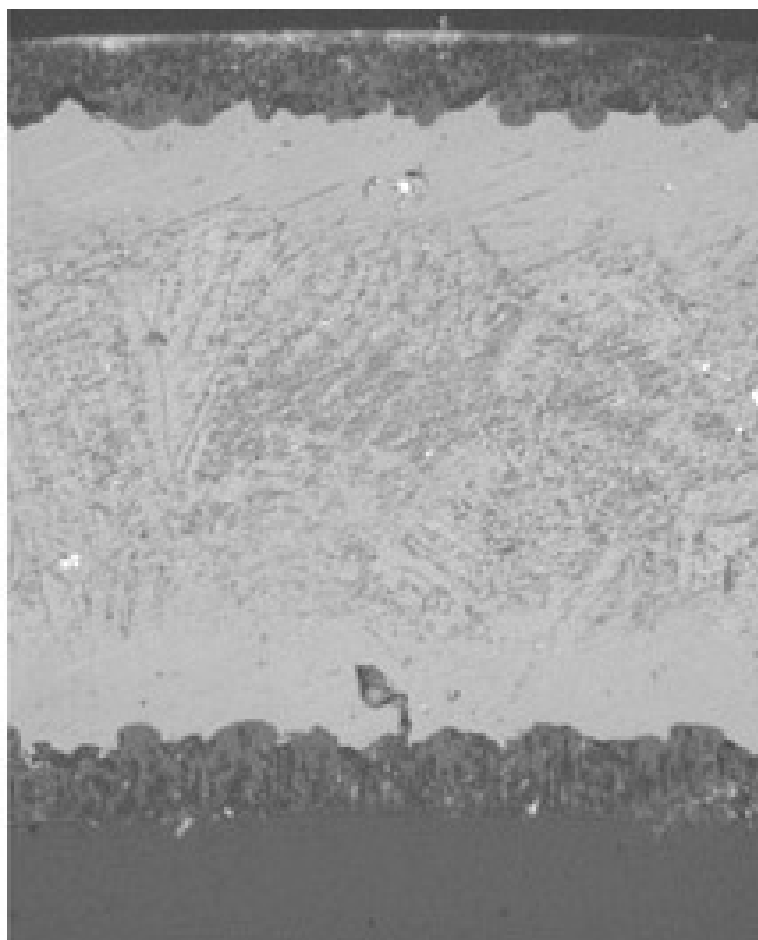
Fig. 7. Post-test appearance of ZIRLO ring-compression samples tested at room temperature and 2 mm/min: (a) samples oxidized at 1000°C; and (b) samples oxidized at 1100°C. ECR values are calculated using the Cathcart-Pawel weight gain correlation.

Table 6 Summary of Characterization of Highly Oxidized Zry-4 and ZIRLO Samples after Exposure to Steam at 1000°C and 1100°C, Slow-cooling to 800°C and Water Quench

Oxidation Temperature °C	Parameter	Zry-4	ZIRLO
1000	Effective Time, s	3364	3364
	Weight Gain, mg/cm <sup>2</sup>	14.6	11.7
	Measured ECR, %	22.4	18.0
	Offset Displacement, mm	0.307	0.271
	Ductility, %	3.2	2.9
	H Content, wppm	19	102
	Hydrogen Pickup, wppm	15	103
	OD/ID Oxide Thickness, μm	83/82	57/66
	Microhardness within Middle 0.2 mm, DPH	290-420	290-400
1100	Effective Time, s	1065	1065
	Weight Gain, mg/cm <sup>2</sup>	13.2	13.7
	Measured ECR, %	20.3	21.1
	Offset Displacement, mm	0.455	0.318
	Ductility, %	4.8	3.3
	H Content, wppm	22	22
	Hydrogen Pickup, wppm	19	18
	Oxide Layer Thickness, μm	70/68	72/69
	Microhardness within Middle 0.2 mm, DPH	240-470	330-460



(a) Zry-4



(b) ZIRLO

Fig. 8. Metallography of as-polished Zry-4 (a) and ZIRLO (b) oxidized in steam at 1000°C for  $\approx 3400$  s, slow cooled to 800°C and water quenched. Measured ECR values are 22.4% for Zry-4 and 18.0% for ZIRLO.

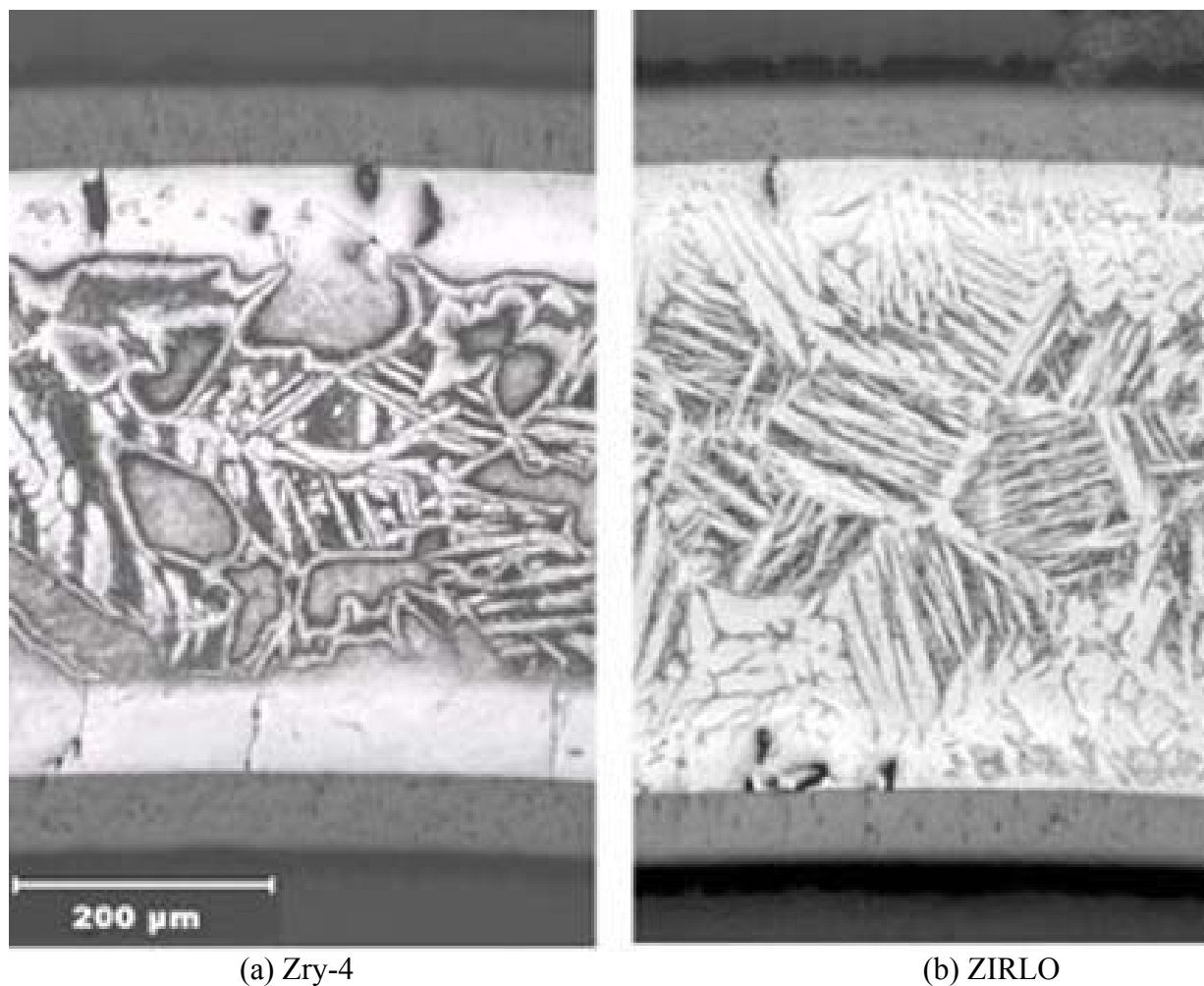


Fig. 9. Metallography of etched Zry-4 (a) and ZIRLO (b) oxidized in steam at  $1100^{\circ}\text{C}$  for  $\approx 1100$  s, slow cooled to  $800^{\circ}\text{C}$  and water quenched. Measured ECR values are 20.3% for Zry-4 and 21.1% for ZIRLO.

#### 4. Summary of Results and Future Work

Weight gain measurements and ring-compression tests have been completed for Zry-4 and ZIRLO cladding-alloy samples, which were oxidized in steam at 1000°C and 1100°C, slow-cooled to 800°C and water quenched. 25-mm-long samples were exposed to two-sided oxidation for test times up to  $\approx 3400$  s at 1000°C and up to  $\approx 1100$  s at 1100°C. The individual test times were chosen to give Cathcart-Pawel (CP) calculated ECR values of 5, 10, 15, 17 and 20%. At 1100°C oxidation temperature, both alloys exhibited about the same weight gain for each of the five test times and were in agreement with CP model predictions. At 1000°C oxidation temperature, the weight gain for ZIRLO was  $>$  Zry-4 for oxidation times  $>1000$  s. Maximum measured ECR values for the 1000°C oxidations were 22.4% for Zry-4 and 18.0% for ZIRLO. Hydrogen pickup was low ( $<25$  wppm) for all samples except for the ZIRLO sample oxidized at 1000°C to 18% ECR ( $\approx 100$  wppm H pickup) and to 17% ECR ( $\approx 35$  wppm). These hydrogen values are most likely too low to influence post-quench ductility.

Ring-compression tests were performed at room temperature and a displacement rate of 2 mm/min. to determine post-quench ductility. The offset displacements determined from the load-displacement curves, normalized to the outer diameter of 9.50 mm, were used as the measure of ductility. Samples with offset strains  $< 2\%$  were classified as brittle. Based on this criterion, all of the samples in the test matrix retained post-quench ductility. Interpretation of the load-displacement curves proved to be very difficult for intermediate-ductility samples. One-to-two minor load drops did not necessarily indicate through-wall failure. Physical examination of the sample and additional displacement-limited tests were needed for these cases. For future testing, it is recommended that two ring compression samples be prepared for each oxidized sample. The ring prepared from 4-to-12 mm from the middle of the sample should be tested to maximum displacement to determine the overall shape of the load displacement curve. If this sample has at least one through-wall crack, the second ring cut from  $\pm 4$  mm from the center should be tested with the displacement limited to the first significant load drop (sharp and large for high-ECR samples and more gradual for some intermediate-ECR samples). For displacement-limited tests, physical examination of the compressed ring can reveal the location and mode of the first through-wall failure, while direct post-test diameter measurements can be performed to support the ductility determined from the offset method.

In addition to hydrogen analysis, post-test characterization consisted of physical examination of all compressed samples, metallographic analysis of the oxidized-and-quenched samples at their highest ECR values, and radial profiling of microhardness for these high-ECR samples. Detailed metallographic and microhardness analyses are in progress to try to correlate the material structure – the amount of low-oxygen content metal remaining after oxidation – with the ring-compression results. Preliminary results are presented in the following. For Zry-4 oxidation at 1100°C to 20% ECR, Fig. 10 shows well defined oxide and oxygen-stabilized (white) alpha layers. The inner and outer oxide and alpha layers are brittle at room temperature as indicated by Vickers hardness measurements  $>1000$  DPH (diamond-pyramid hardness). The alpha incursions, slightly grayer than the alpha layers that formed at 1100°C, have a Vickers hardness of  $\approx 500$  DPH, indicating that they probably formed at lower oxygen content during cooling from 1100°C to 800°C prior to quench. The gray-white and gray regions within what was the beta layer at 1100°C contain intermediate-to-low oxygen content regions. The microhardness of this mixed region is  $\approx 300$  DPH. This microhardness is consistent with values

reported by Hobson and Rittenhouse [5] and Hobson [6] for the prior-beta layer after oxidation at 1066-1093°C and rapid cooling. This microhardness is low enough and the dark gray region is extensive enough to support ductile behavior in the ring-compression tests.

The ring-compression results for samples oxidized at 1000°C for  $\approx 3400$  s, prior to quench, are very interesting in that the post-quench ductility values for both alloys are  $\approx 3\%$  even though the weight gains are different. The results in Table 6 show that the weight-gain values scale with the oxide-layer-thickness values. However, to understand whether or not the alloys should behave in a ductile manner, it is important to examine their microstructures and radial profiles of microhardness. In Fig. 11, the etched microstructure of ZIRLO is shown after oxidation for  $\approx 3400$  s at 1000°C. It shows that the oxygen-stabilized alpha layers are less well defined than for Zry-4 and that the prior beta layer is now a more complicated mixture of phases, most likely with varying levels of oxygen. As indicated in Table 6, microhardness values as low as  $\approx 330$  DPH were found near the middle of the ZIRLO sample – comparable to those for Zry-4. However, it is difficult to quantify the extent of the low-oxygen-content ductile material for ZIRLO, especially as the phase diagram for this alloy has not been characterized very well in open literature publications. More work is in progress to correlate microstructure with post-quench ductility.

In summary, the ring-compression test appears to be a reasonable screening test for post-quench ductility, especially for comparing the performance of alloys oxidized and tested under the same conditions. However, the “ductility” determined in this study, does not represent a material property as well defined as tensile-test uniform elongation. The ring-compression hoop bending stresses and strains, as well as the alpha incursions that lead to ductility decrease, are not uniform in the circumferential direction. Different quantitative results would have been obtained with changes in oxidation (one-sided vs. two-sided), changes in sample cooling rate (quench from oxidation temperature vs. quench from 800°C), changes in load-support design (curved vs. flat), and changes in ring-compression test conditions (strain rate and temperature). Also, the demonstration of ductility in non-deformed rings with very little hydrogen pick-up does not guarantee that ballooned-and-burst cladding with corrosion-induced hydrogen pickup and/or with secondary hydriding from inner-surface oxidation would behave in a ductile manner.

Future work consists of completing the test matrix for the 1200°C and 1260°C oxidation temperatures and completing the correlation between ring-compression ductility and microstructure/chemistry of the alloys. The 1200°C Zry-4 and ZIRLO samples have been prepared and will be subjected to ring compression tests in the very near future. Work is in progress to prepare both alloys at 1260°C. ZIRLO and Zry-4 LOCA integral tests will be performed at 1000°C, 1100°C and 1200°C and 17% ECR (calculated). Such tests would generate samples with a ballooned-and-burst region and with secondary hydriding in the neck and beyond-neck regions. The ANL-proposed method of determining post-quench ductility is to subject the LOCA post-quench samples to a four-point-bend-test, followed by ring compression tests for 8-mm-long rings cut from the beyond-neck region.

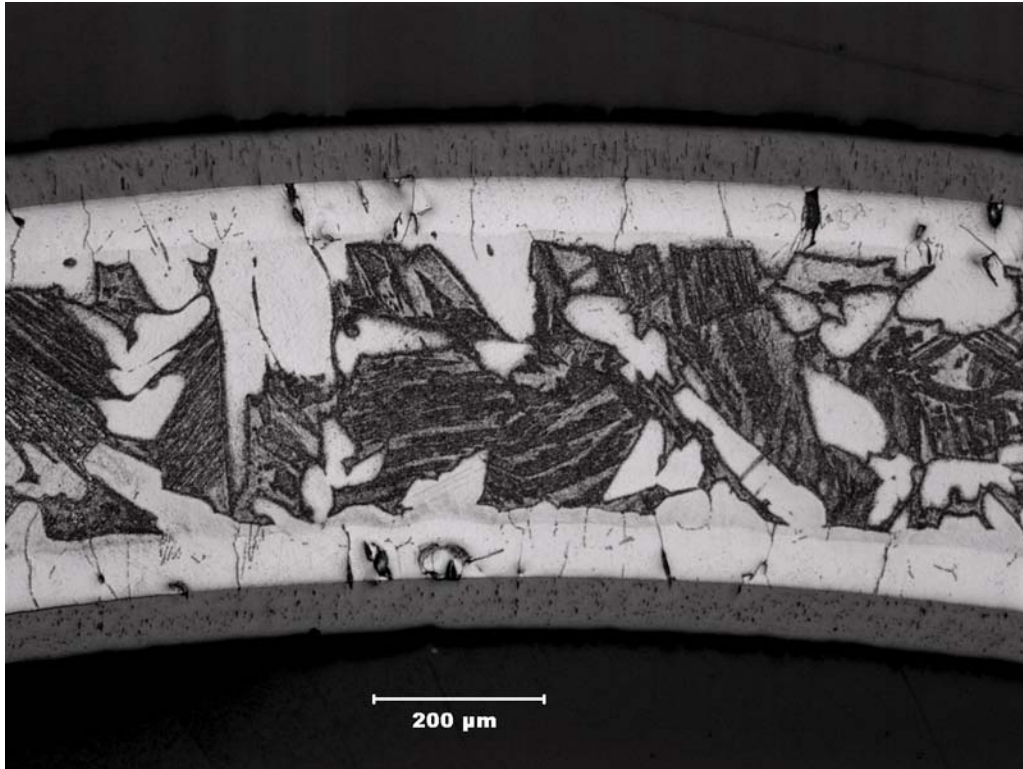


Fig. 10. Microstructure of etched Zry-4 after oxidation at 1100°C for  $\approx 1100$  s, slow cooling to 800°C and quench. Microhardness values of the oxide and oxygen-stabilized alpha (light gray) layers are  $>1000$  DPH, while microhardness of the alpha incursions (slightly darker gray) is  $\approx 500$  DPH and microhardness of the low-oxygen, prior-beta layer (dark gray) is  $\approx 300$  DPH.

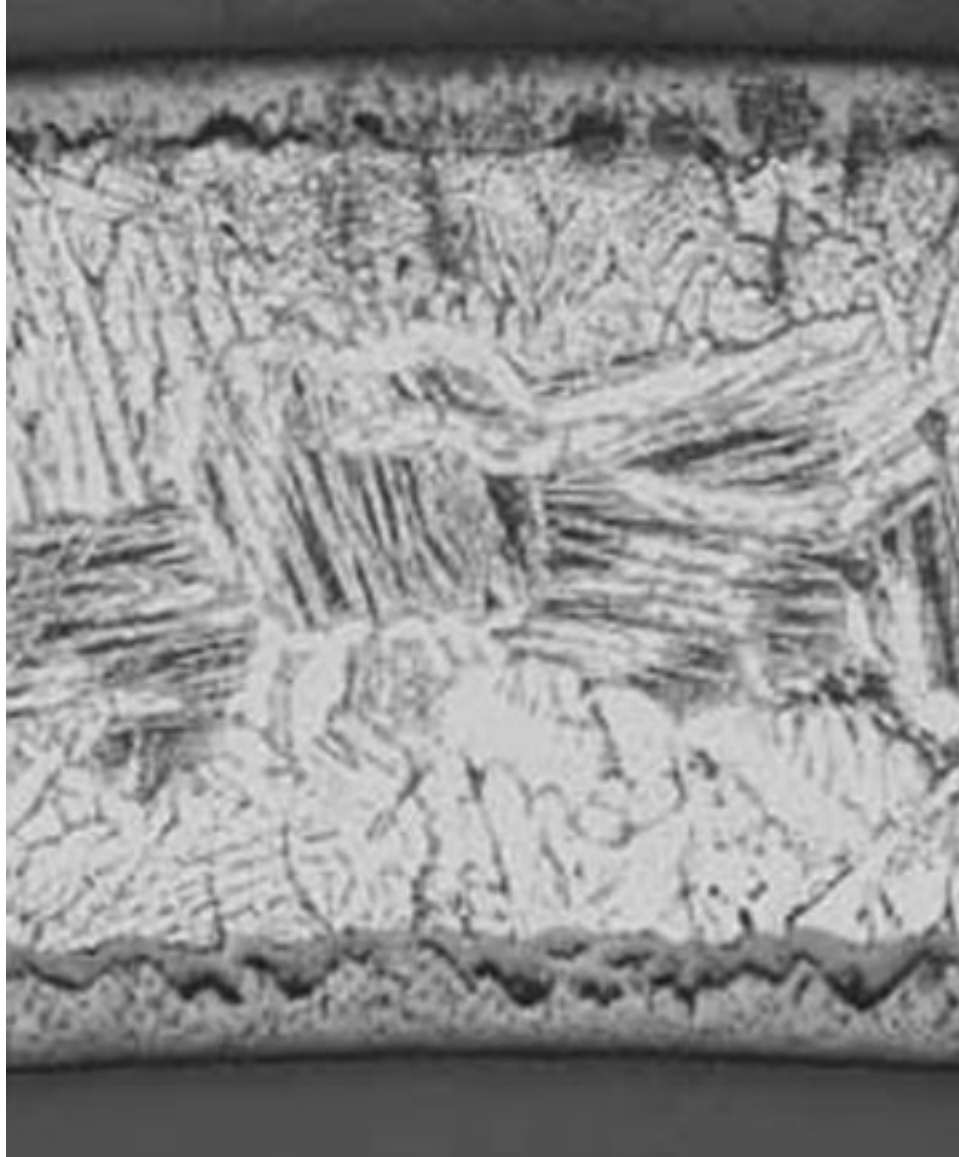


Fig. 11. Microstructure of etched ZIRLO after oxidation for  $\approx 3400$  s at  $1000^{\circ}\text{C}$ , slow cooling to  $800^{\circ}\text{C}$  and quench.



## References

1. Y. Yan, T. Burtseva and M. C. Billone, "Validation Test Results for M5 Post-Quench-Ductility Sample Preparation," letter report to NRC and Framatome, April 8, 2003.
2. Y. Yan, T. Burtseva and M. C. Billone, "Progress Report on Sample Preparation for Post-Quench-Ductility Tests of Westinghouse Zircaloy-4 and ZIRLO," letter report to NRC and Westinghouse, April 11, 2003.
3. Y. Yan, T. Burtseva and M. C. Billone, "Progress Report on E110 Post-Quench Ductility Test Program," letter report to NRC and RRC KI, May 31, 2003.
4. M. C. Billone, T. Burtseva and Y. Yan, "Hydrogen Pickup and Ring-Compression Ductility for E110 Oxidized in Steam at 1000°C," letter report to NRC and RRC KI, January 19, 2004.
5. D. O. Hobson and P. L. Rittenhouse, "Embrittlement of Zircaloy-Clad Fuel Rods by Steam during LOCA Transients," ORNL 4758, January 1972.
6. D. O. Hobson, "Ductile-Brittle Behavior of Zircaloy Fuel Cladding," Proc. ANS Topical Mtg. on Water Reactor Safety, Salt Lake City, March 26, 1973, pp. 274-288.

## **APPENDIX A**

### **Load-Displacement Curves for Oxidized-and-Quenched Zry-4 Samples Subjected to Ring-Compression Tests at Room Temperature and a Cross-head Displacement Rate of 2 mm/minute**

**Note: ECR values listed on the figures are approximate values. For more precise values, refer to Tables 4 and 5 in the main body of the report.**

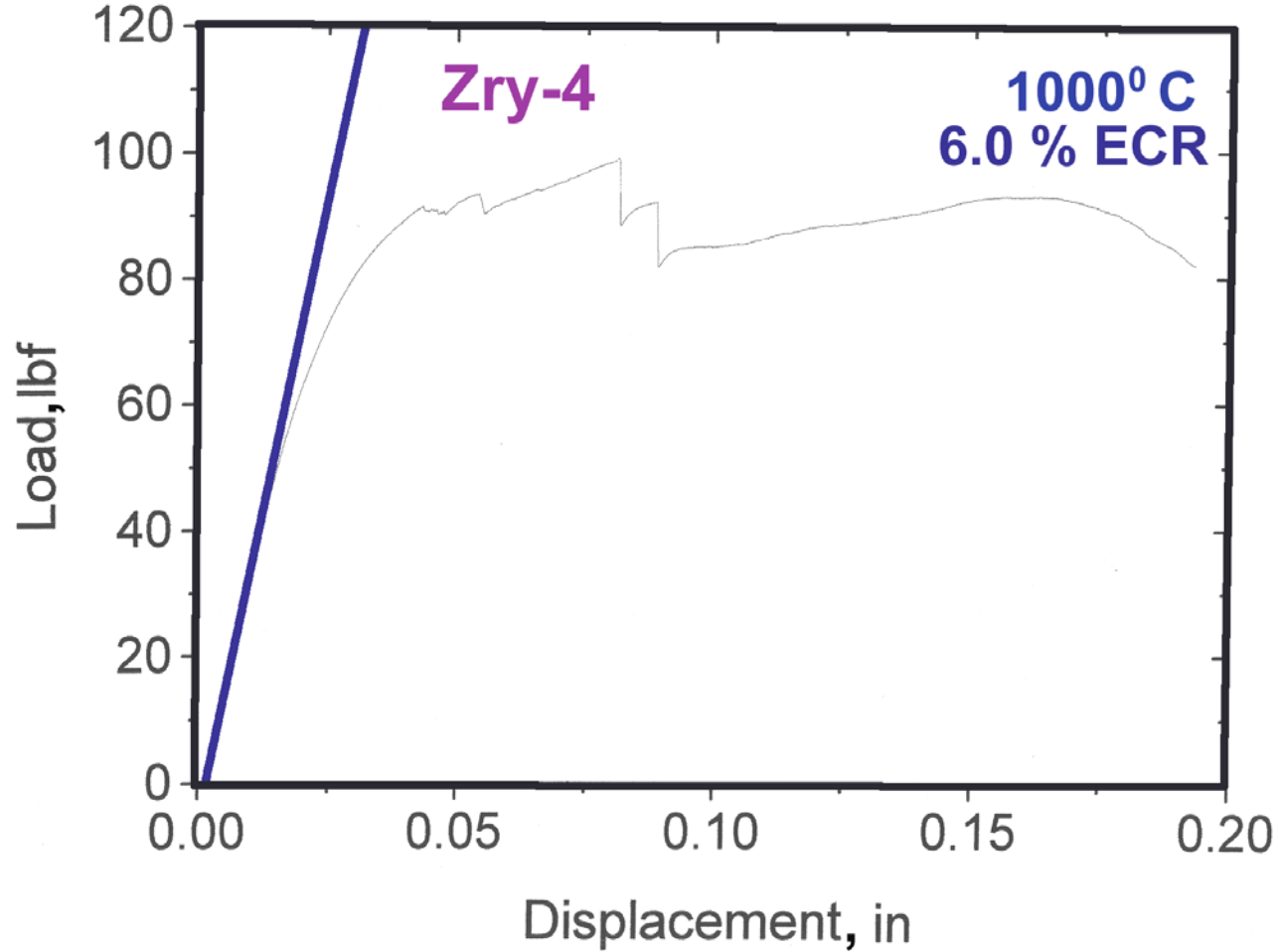


Fig. A.1 Ring-compression load-displacement data for Zry-4 oxidized to  $\approx 6\%$  ECR at  $1000^{\circ}\text{C}$ . Sample was intact; no through-wall crack observed. Significant buckling observed. Oxide/ $\alpha$  cracking, which should correspond to the two load drops, observed on buckled outside surface. Offset displacement of 4.4 mm was determined from the end point of the curve.

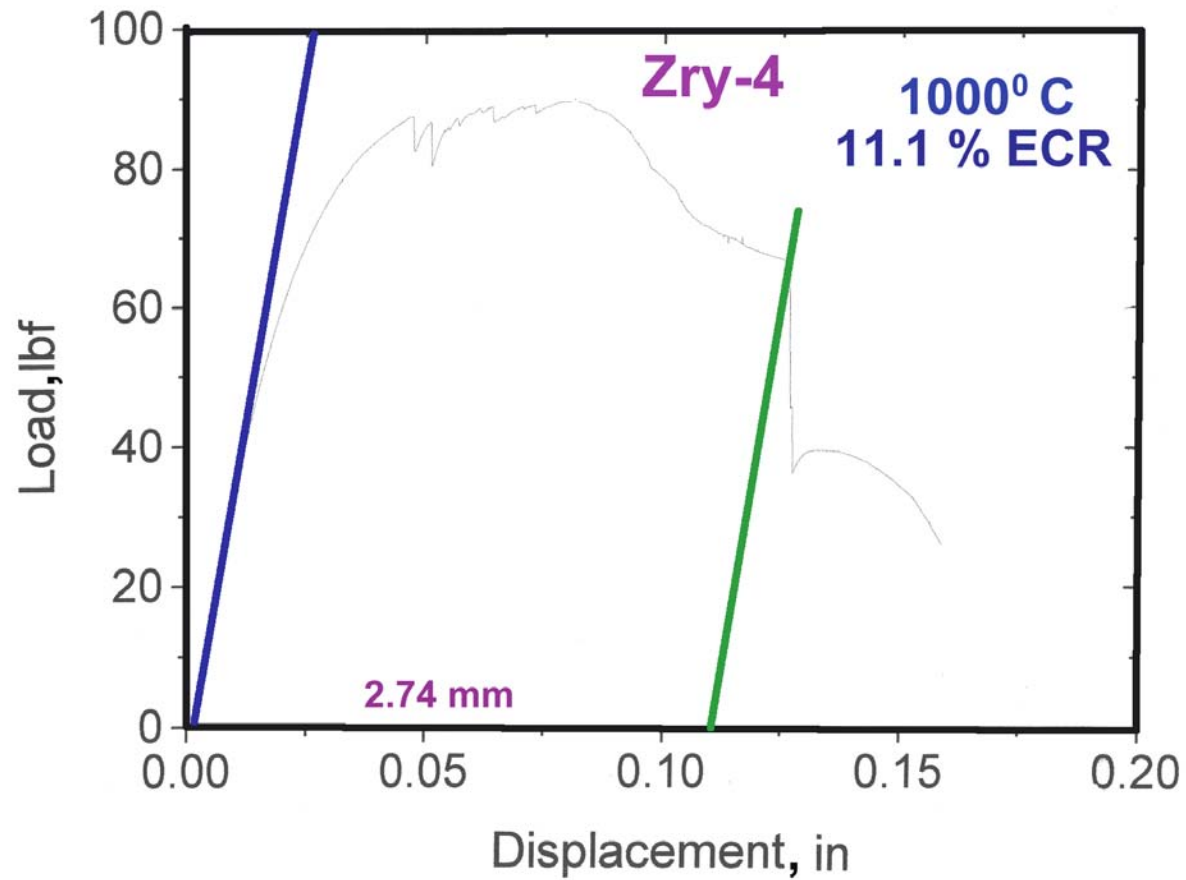


Fig. A.2 Ring-compression load-displacement data for Zry-4 oxidized to  $\approx 11\%$  ECR at  $1000^{\circ}\text{C}$ . One through-wall crack, corresponding to large abrupt load drop, observed in buckled region. Local ductility in this buckled region is much higher than the 29% calculated from the 2.74 mm offset displacement.

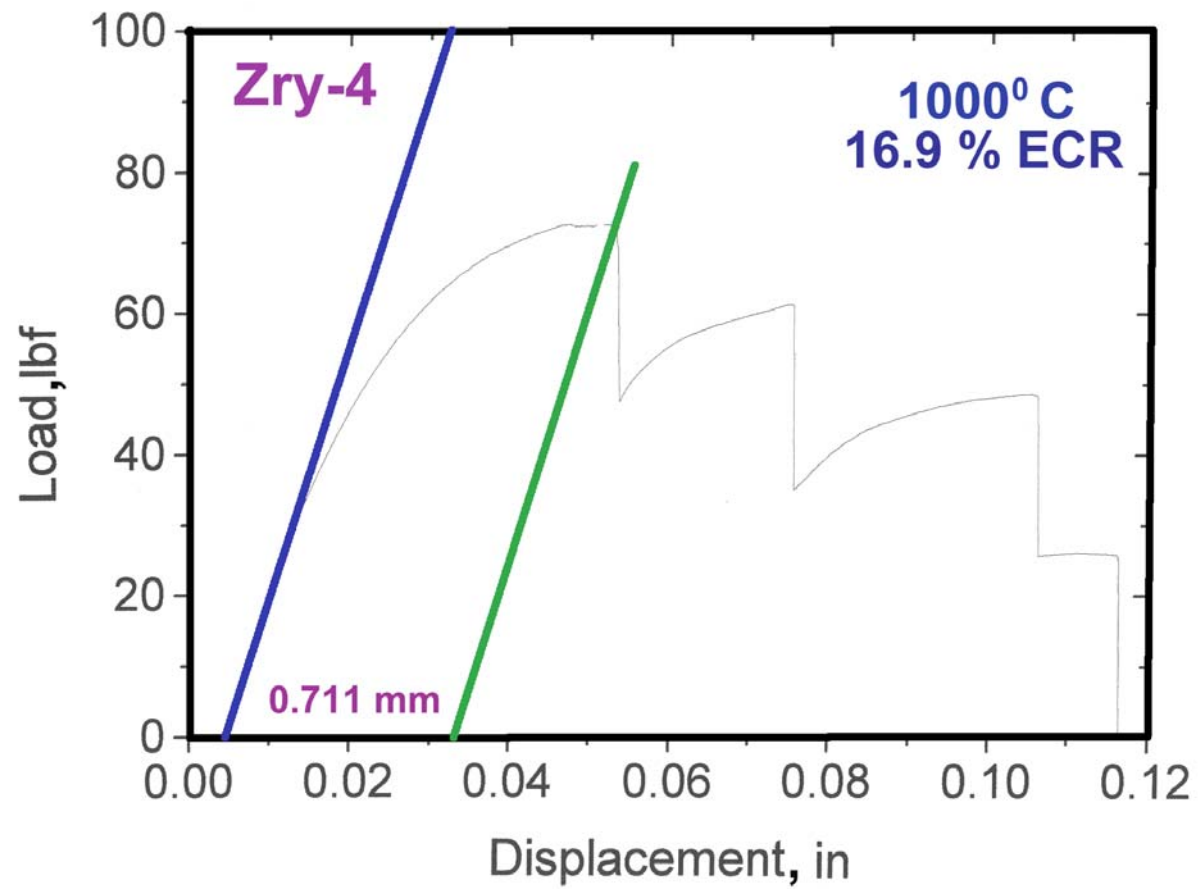


Fig. A.3 Ring-compression load-displacement data for Zry-4 oxidized to  $\approx 17\%$  ECR at  $1000^{\circ}\text{C}$ . Four through-wall cracks observed.

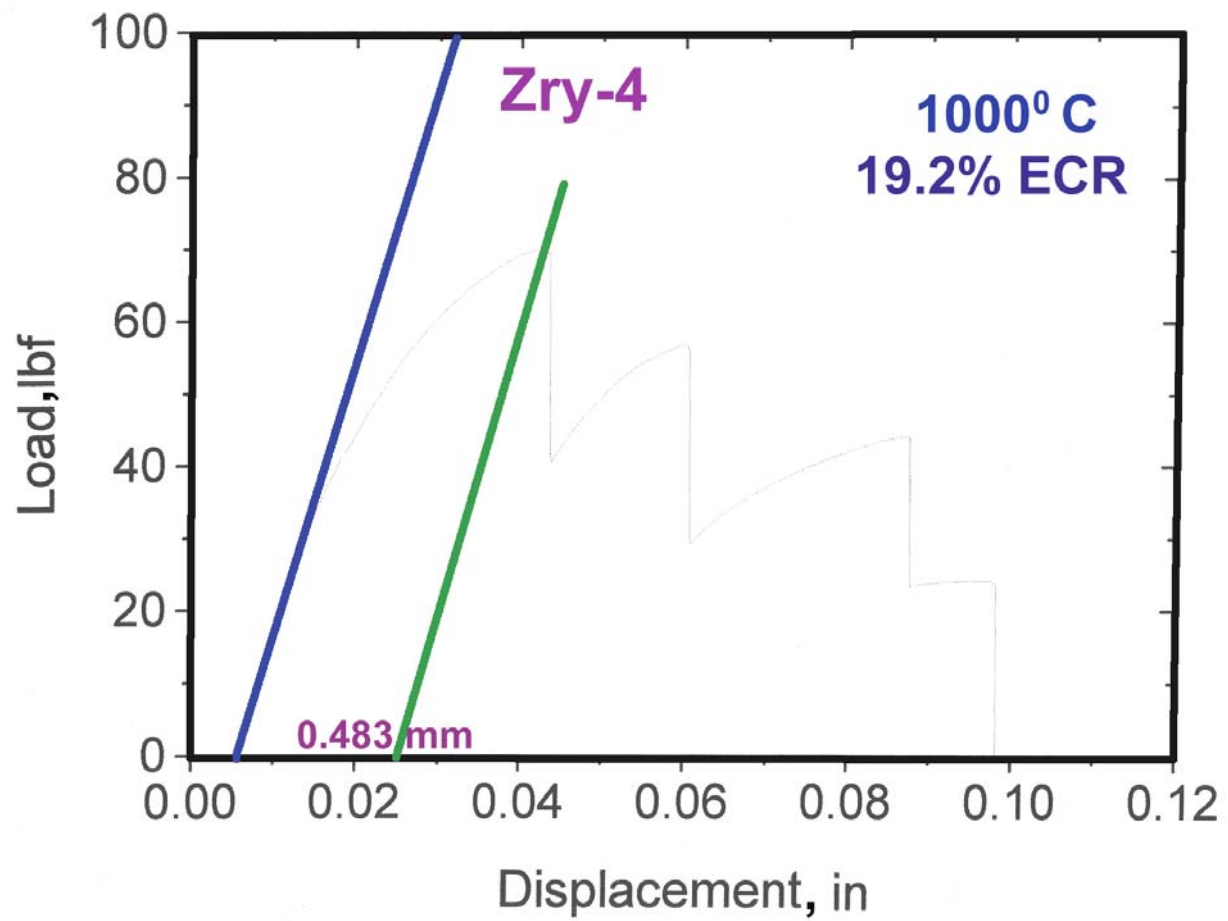


Fig. A.4 Ring-compression load-displacement data for Zry-4 oxidized to  $\approx 19\%$  ECR at  $1000^{\circ}\text{C}$ . Four through-wall cracks observed.

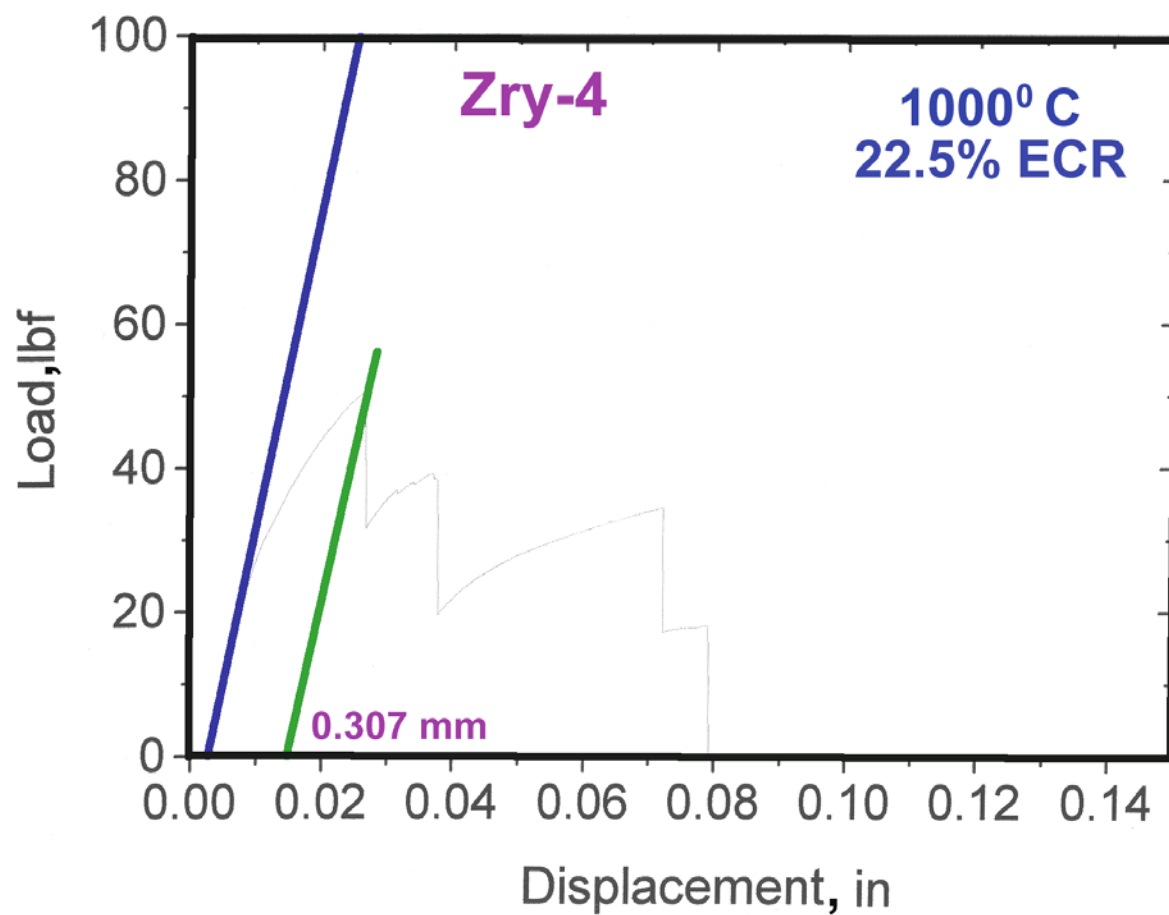


Fig. A.5 Ring-compression load-displacement data for Zry-4 oxidized to  $\approx 22\%$  ECR at  $1000^{\circ}\text{C}$ . Four through-wall cracks observed.

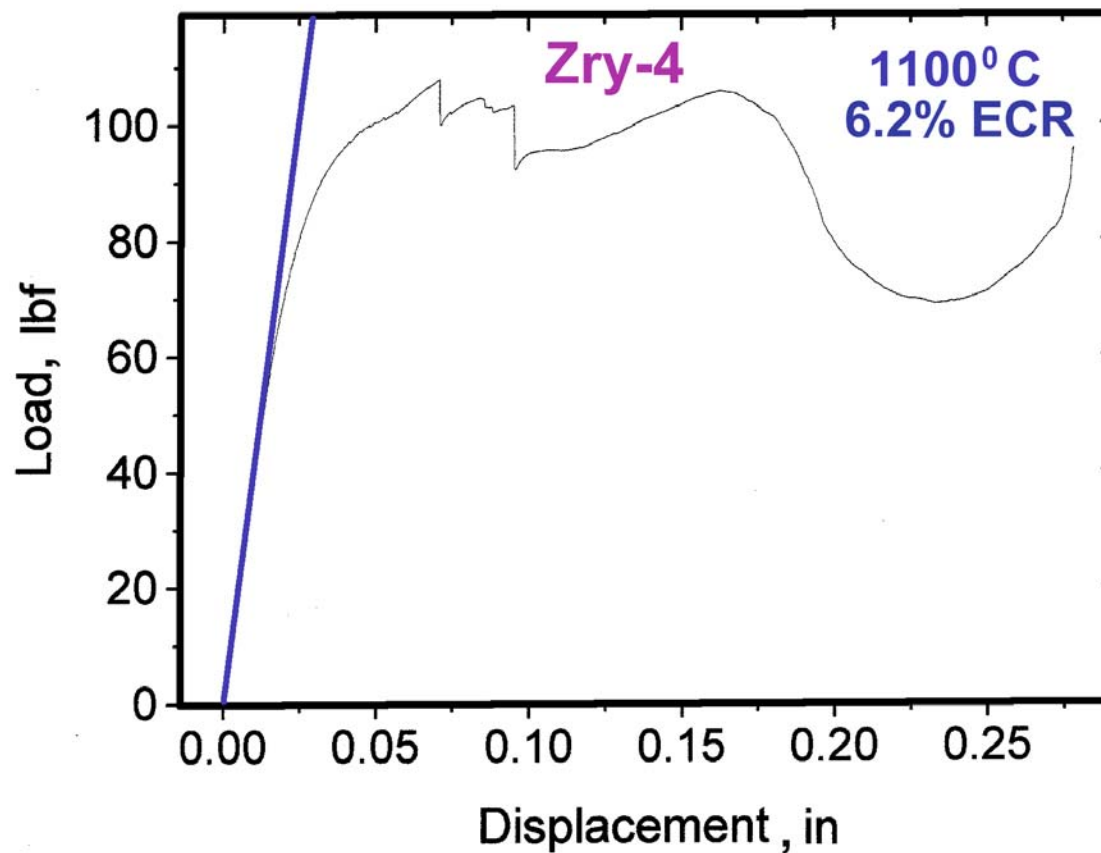


Fig. A.6 Ring-compression load-displacement data for Zry-4 oxidized to  $\approx 6\%$  ECR at  $1100^{\circ}\text{C}$ . Sample intact; no through-wall crack. Significant buckling observed. Oxide/alpha cracking, which should correspond to the two load drops, observed on buckled outside surface. Offset displacement of 5.5 mm was determined by “unloading” from the point at 0.225” on the displacement axis prior to the upswing in load.



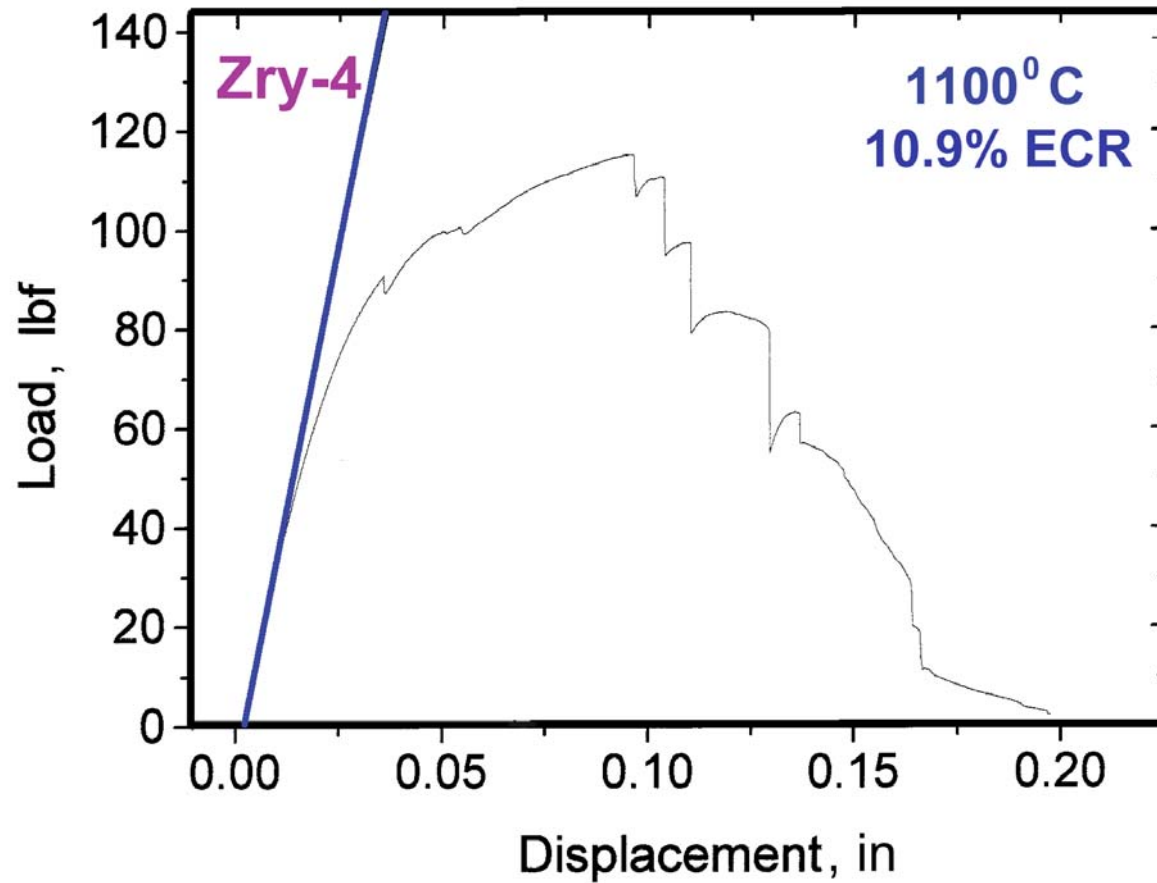


Fig. A.7 Ring-compression load-displacement data for Zry-4 oxidized to  $\approx 11\%$  ECR at  $1100^{\circ}\text{C}$ . Three through-wall cracks and one partial-wall crack were observed. The first through-wall crack is associated with the second load drop, which corresponds to an offset displacement of 1.9 mm.

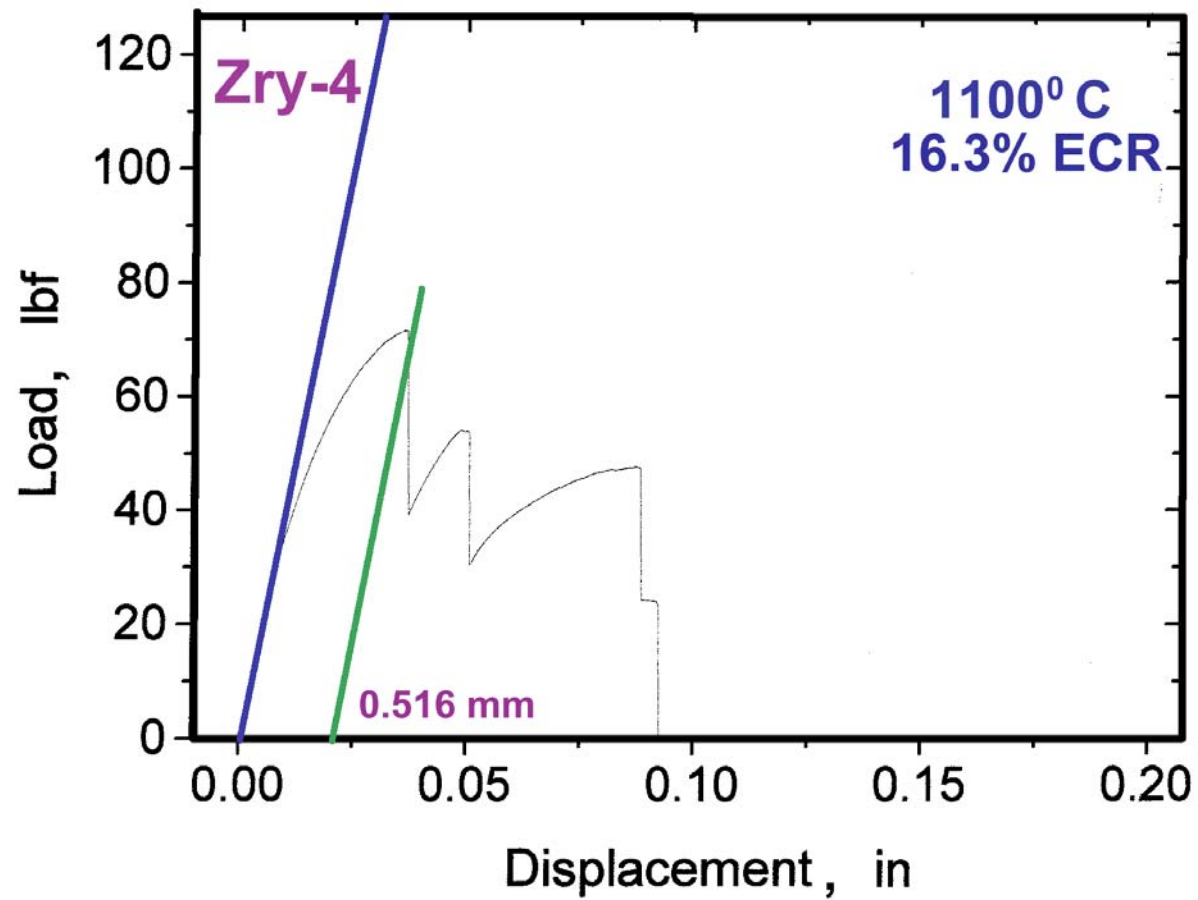


Fig. A.8 Ring-compression load-displacement data for Zry-4 oxidized to  $\approx 16\%$  ECR at  $1100^{\circ}\text{C}$ . Sample fractured into four pieces with no evidence of buckling.

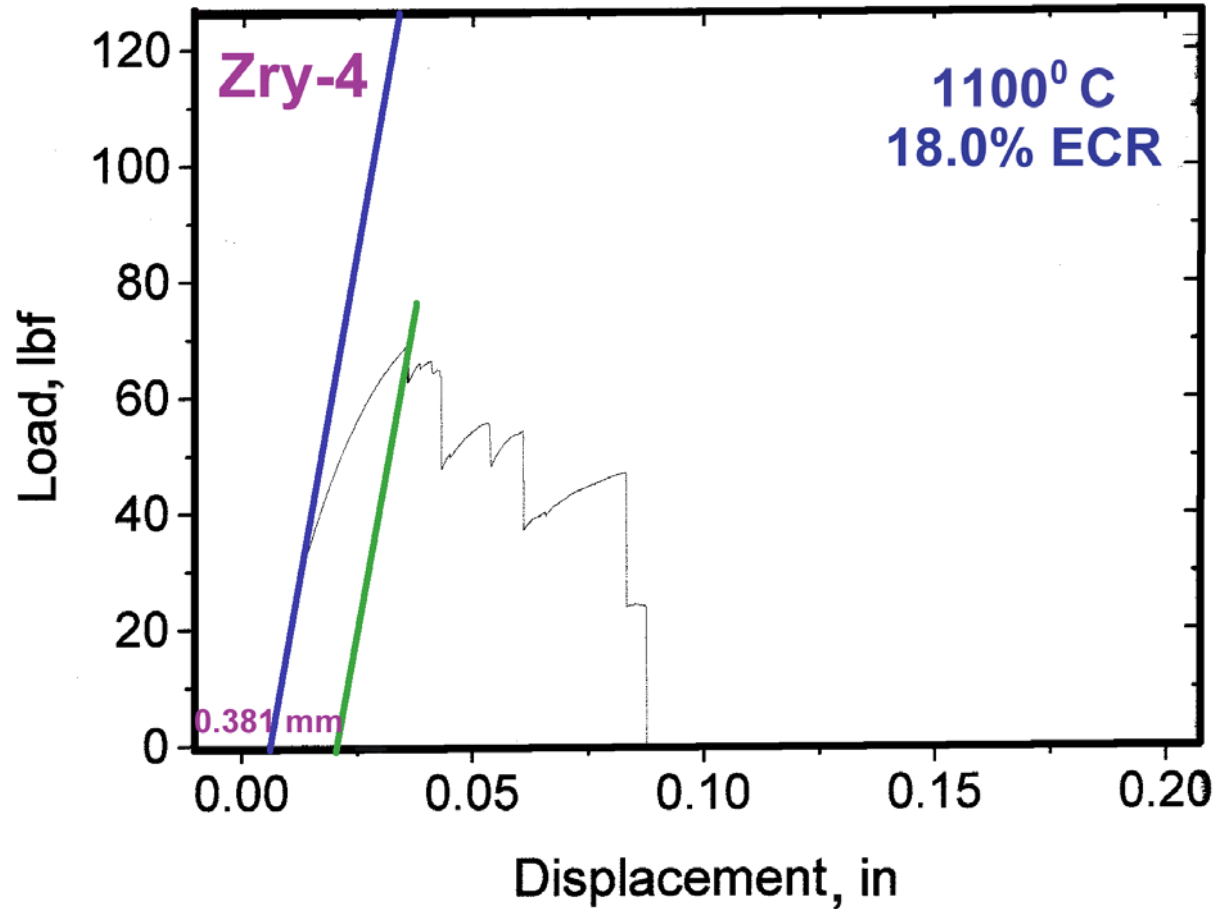


Fig. A.9 Ring-compression load-displacement data for Zry-4 oxidized to  $\approx 18\%$  ECR at  $1100^{\circ}\text{C}$ . Sample fractured into 3 pieces. First through-wall crack likely developed at second load-drop, with an offset displacement of 0.56 mm. However, some of the apparent offset between 0.38 and 0.56 mm is due to crack displacement, rather than plastic deformation.

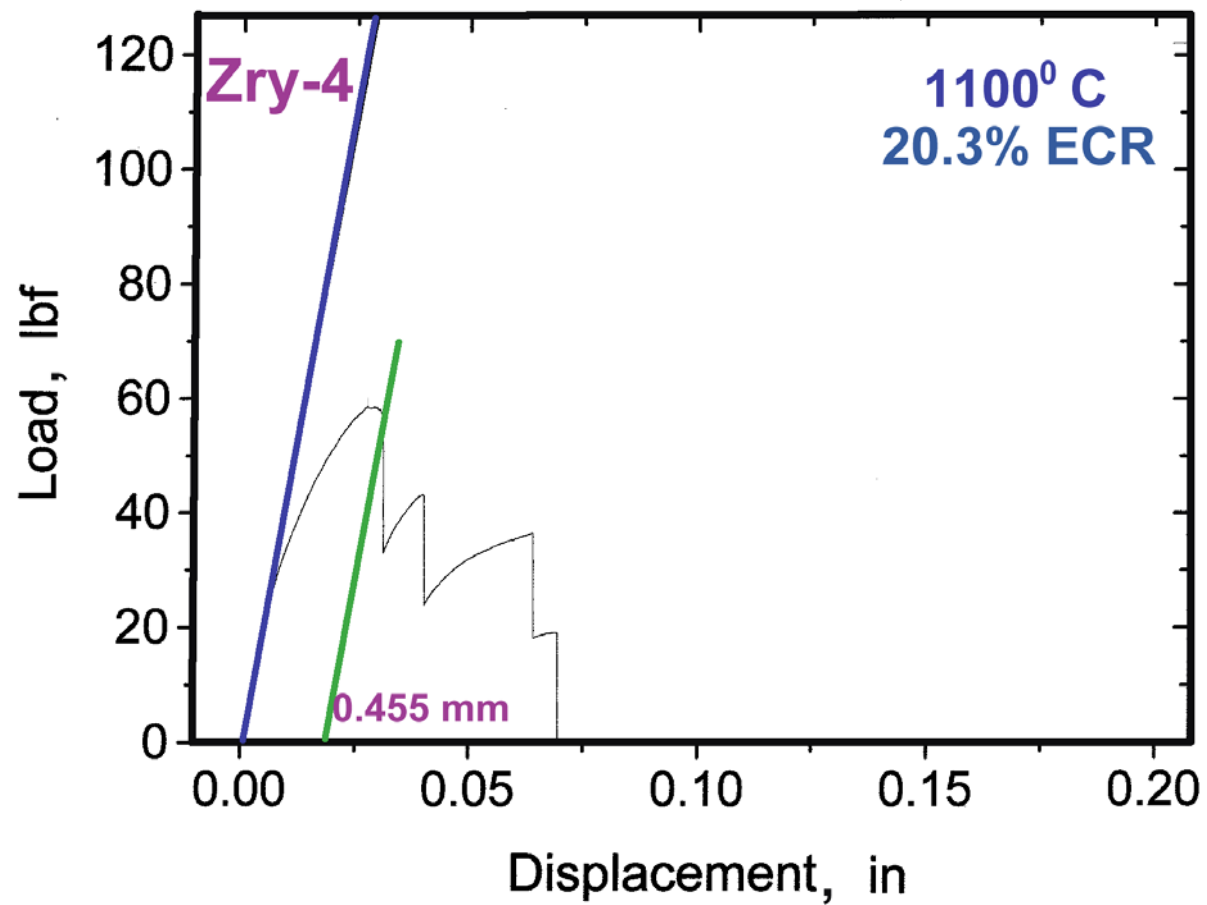


Fig. A.10 Ring-compression load-displacement data for Zry-4 oxidized to  $\approx 20\%$  ECR at  $1100^{\circ}\text{C}$ . Sample fractured into four pieces, corresponding to the four load drops.

## **APPENDIX B**

### **Load-Displacement Curves for Oxidized-and-Quenched ZIRLO Samples Subjected to Ring-Compression Tests at Room Temperature and a Cross-head Displacement Rate of 2 mm/minute**

**Note: ECR values listed on the figures are approximate values. For more precise values, refer to Tables 4 and 5 in the main body of the report.**

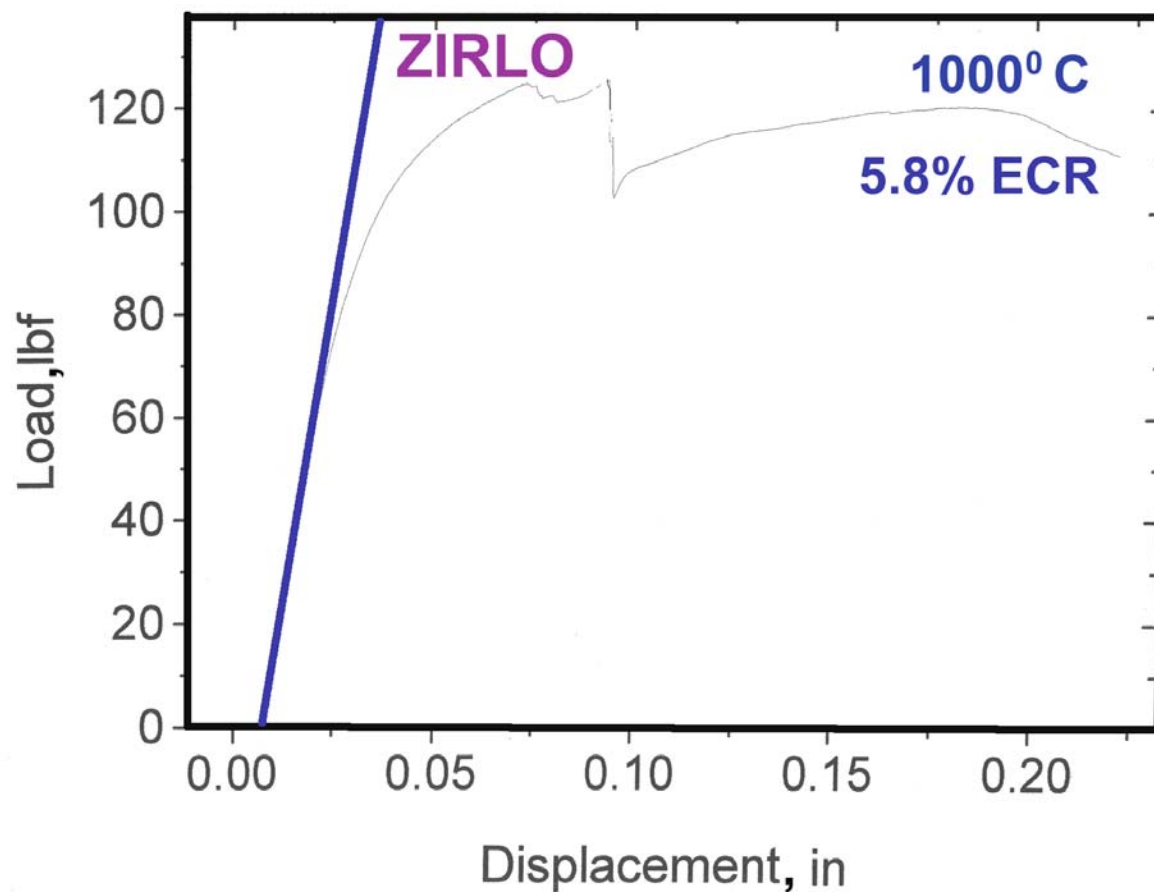


Fig. B.1 Ring-compression load-displacement data for ZIRLO oxidized to  $\approx 6\%$  ECR at  $1000^{\circ}\text{C}$ . Sample intact; no through-wall crack. Significant buckling. Oxide/alpha cracking, which should correspond to the one sudden load drop, observed on buckled outside surface. Offset displacement (4.9 mm) is determined by unloading from the end of the curve with the same slope as the blue line.

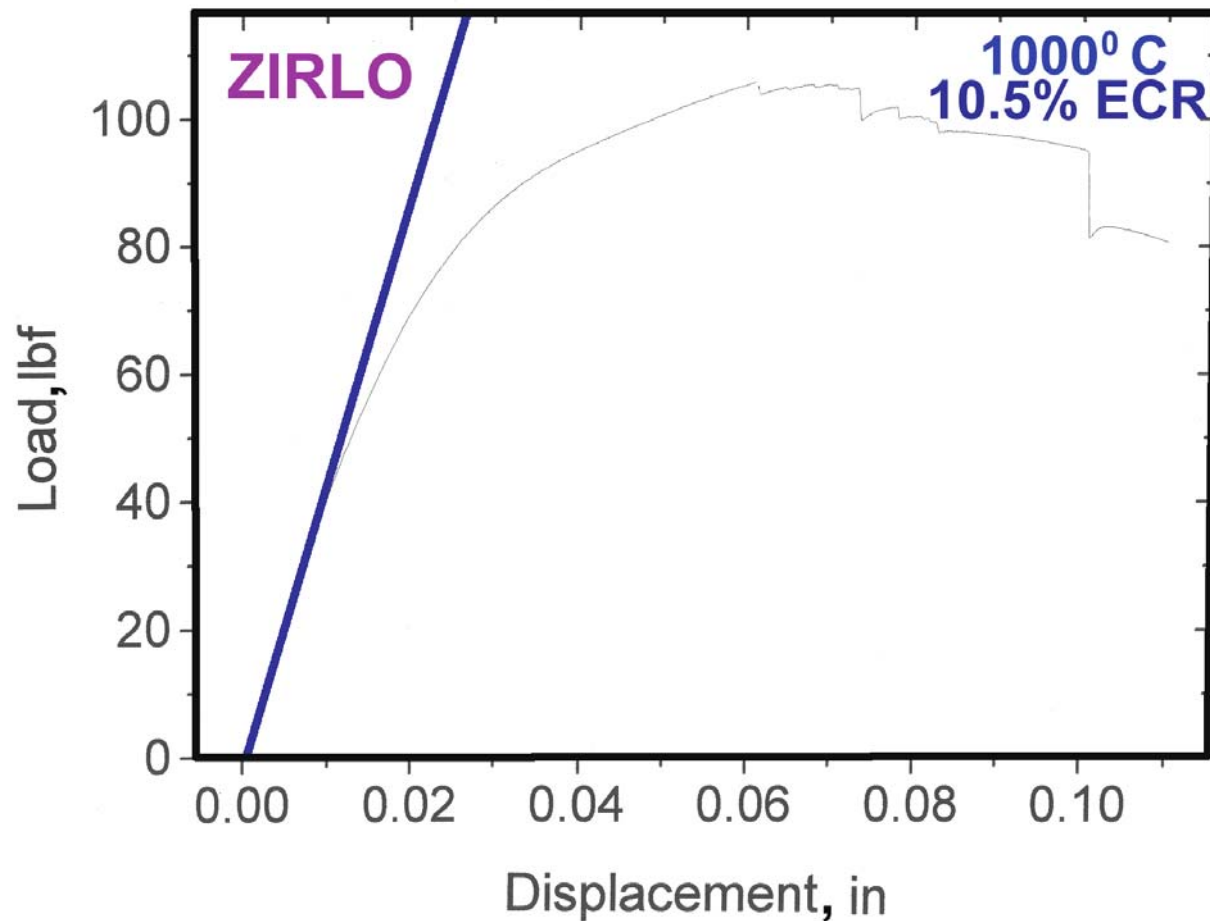


Fig. B.2 Ring-compression load-displacement data for ZIRLO oxidized to  $\approx 11\%$  ECR at  $1000^{\circ}\text{C}$ . Sample intact; no through-wall crack. Significant buckling. Oxide/ $\alpha$  cracking, which should correspond to the sudden load drop, observed on buckled outside surface of top and bottom buckled regions. Offset displacement (2.35 mm) is determined by unloading from the end of the curve with the same slope as the blue line.

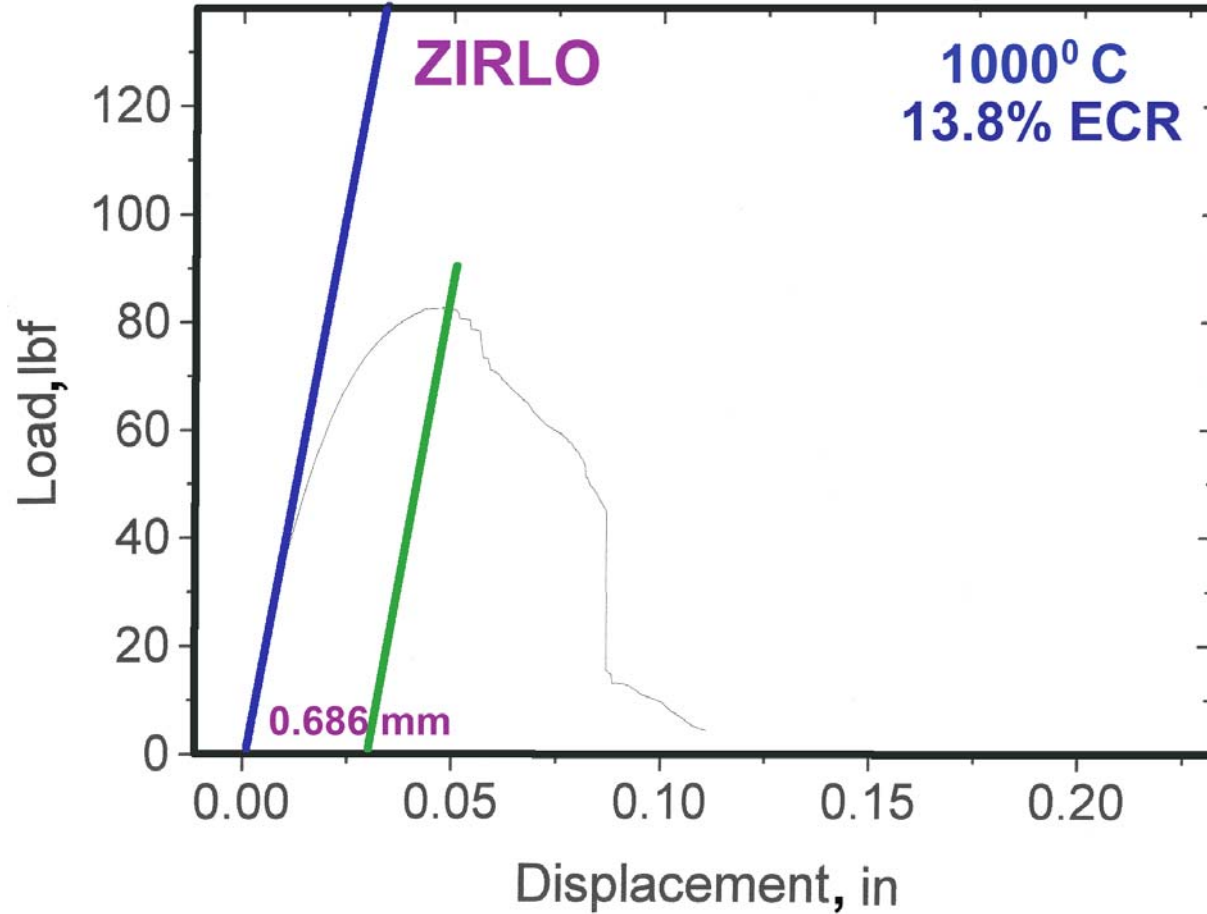


Fig. B.3 Ring-compression load-displacement data for ZIRLO oxidized to  $\approx 14\%$  ECR at  $1000^{\circ}\text{C}$ . One through-wall crack observed, corresponding to large abrupt load drop at 1.92 mm offset. Through wall crack is  $90^{\circ}$  from load application point. Mild buckling observed. Partial-wall crack observed at load-application or support surface. Through-wall crack at this location occurred during handling at very low manual load (see Fig. 7a). The green line at 0.686 mm offset was only used as a reference line.



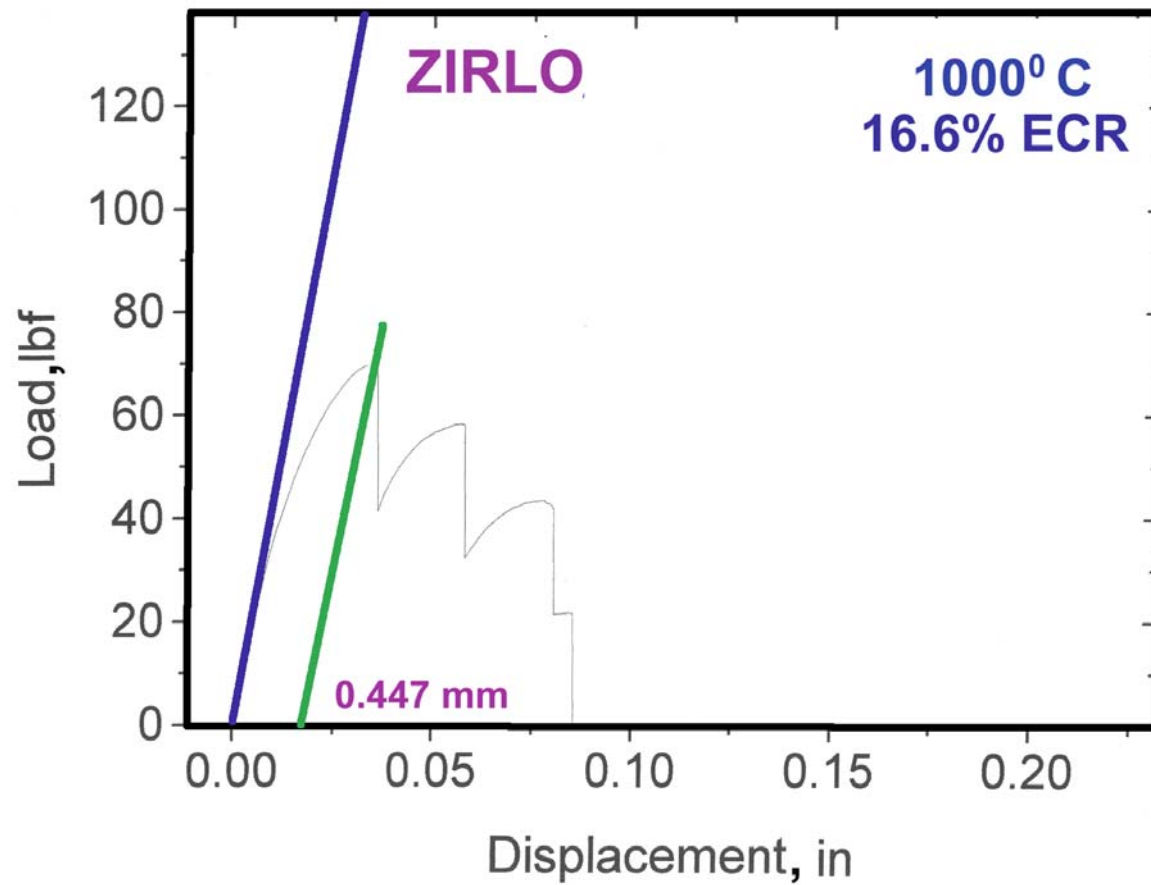


Fig. B.4 Ring-compression load-displacement data for ZIRLO oxidized to  $\approx 17\%$  ECR at  $1000^{\circ}\text{C}$ . Sample broke into four pieces corresponding to the four load drops.

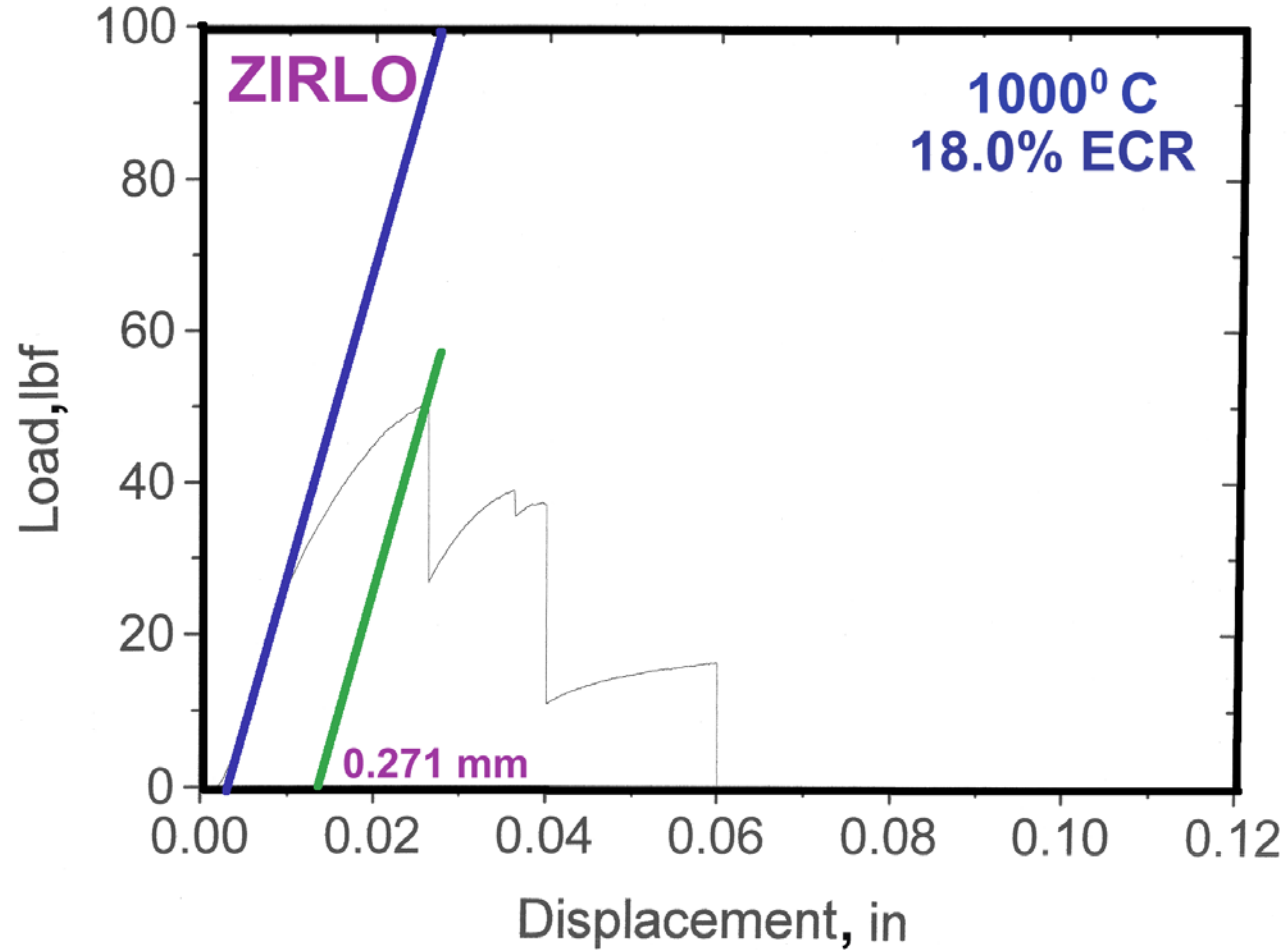


Fig. B.5 Ring-compression load-displacement data for ZIRLO oxidized to  $\approx 18\%$  ECR at  $1000^\circ\text{C}$ . Sample fractured into four pieces; only 3 were recovered after the test (see Fig. 7a).

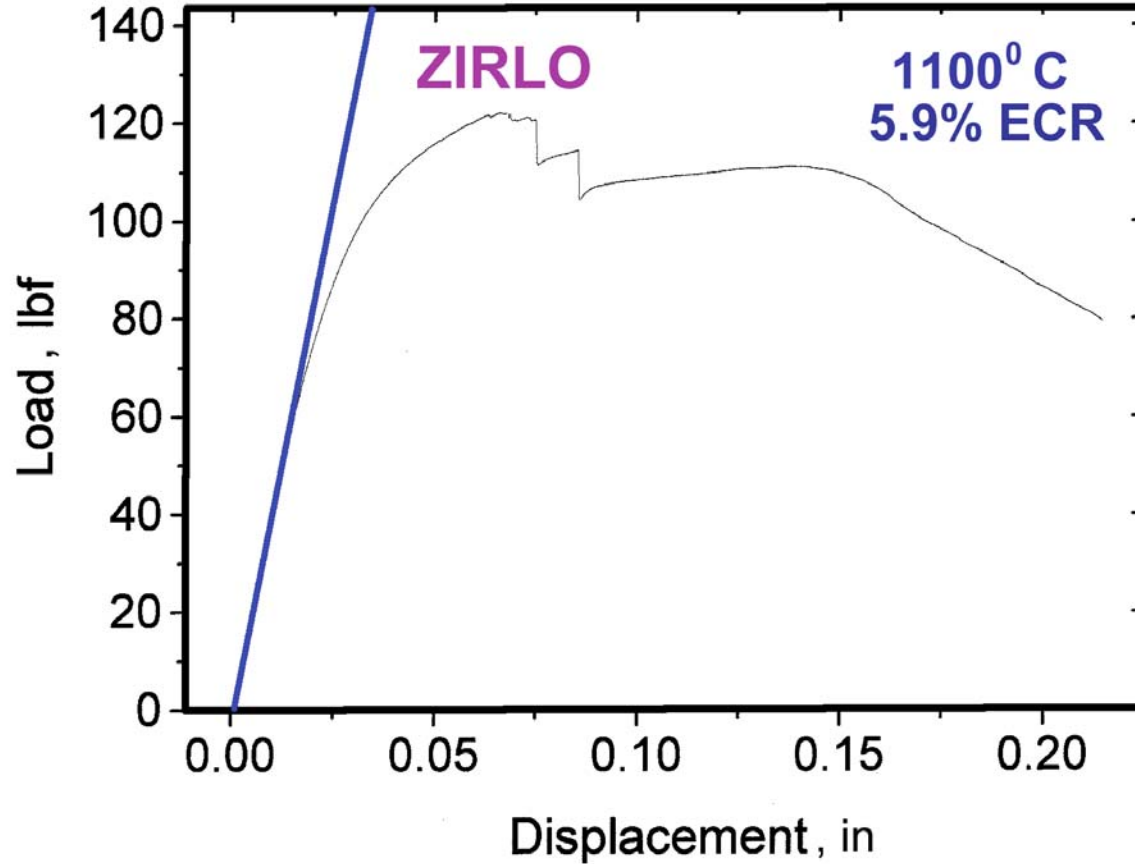


Fig. B.6 Ring-compression load-displacement data for ZIRLO oxidized to  $\approx 6\%$  ECR at  $1100^{\circ}\text{C}$ . Sample intact; no through-wall crack. Significant buckling. Oxide/alpha cracking, which should correspond to the two load drops, observed on buckled outside surfaces of buckled regions. The offset displacement (5.0 mm) was determined by unloading at the slope of the blue line from the end of the curve.

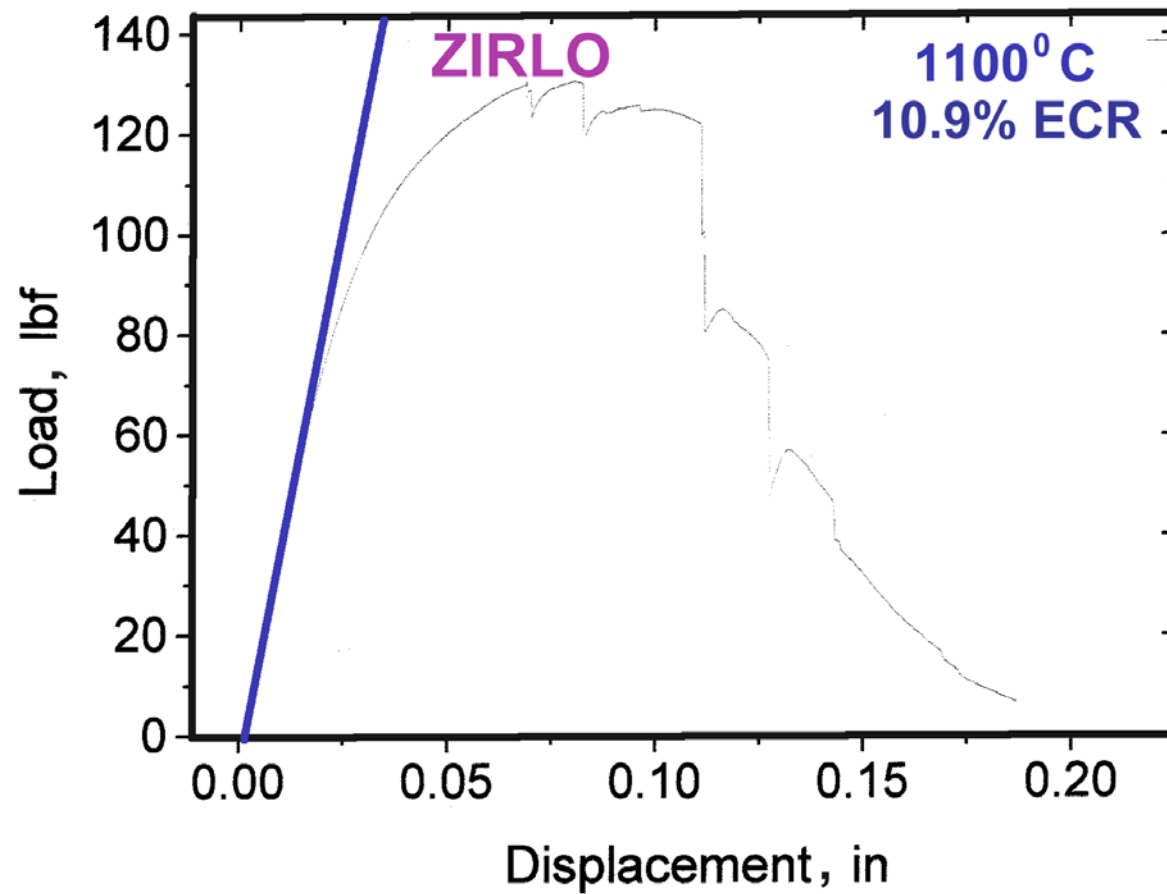


Fig. B.7 Ring-compression load-displacement data for ZIRLO oxidized to  $\approx 11\%$  ECR at  $1100^{\circ}\text{C}$ . Two through wall cracks through top and bottom buckled regions (see Fig. 7b). Offset displacement (2.1 mm) is based on unloading just prior to the  $\approx 40$  lbf load drop.

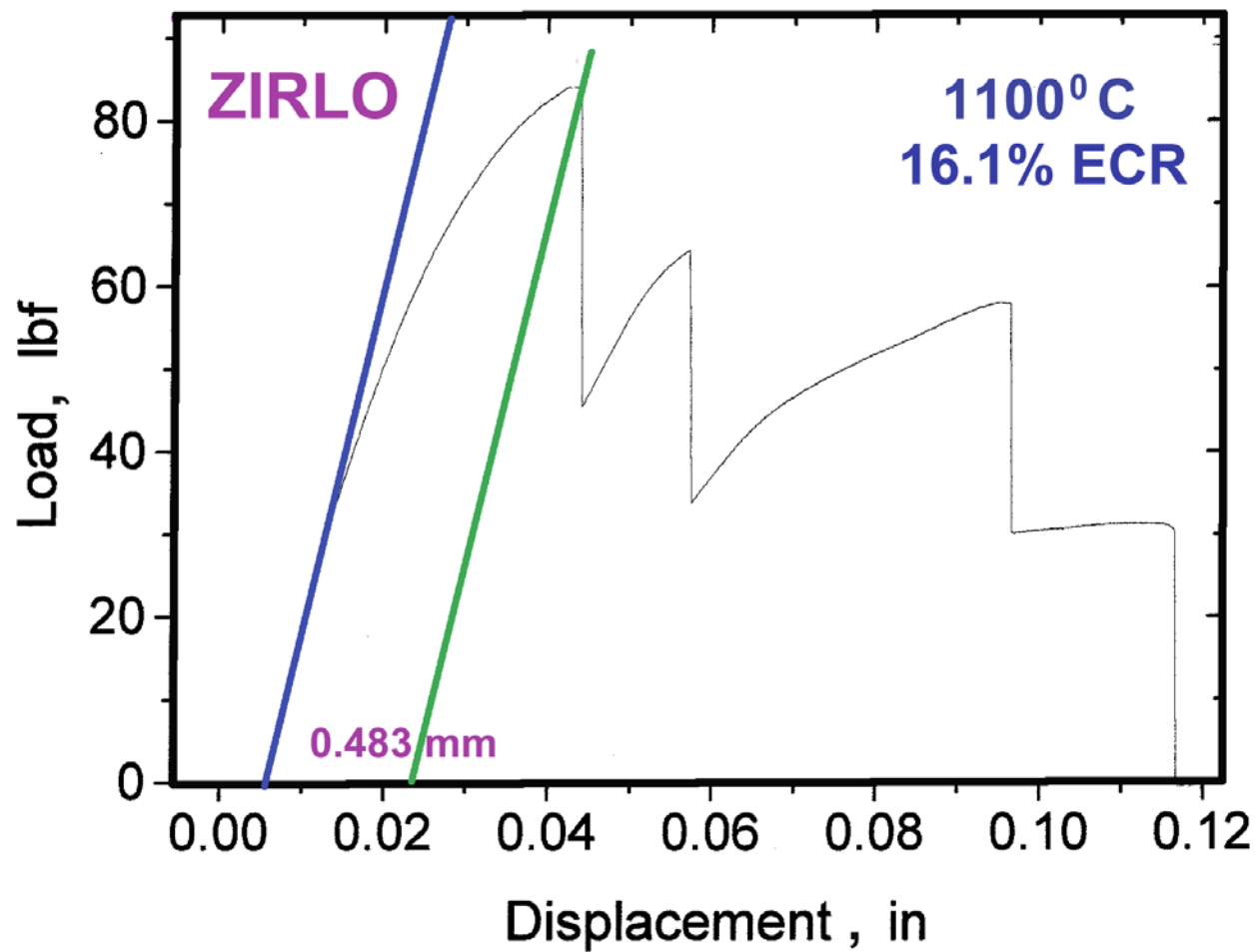


Fig. B.8 Ring-compression load-displacement data for ZIRLO oxidized to  $\approx 16\%$  ECR at  $1100^{\circ}\text{C}$ . Sample fractured into four pieces, corresponding to the load drops.

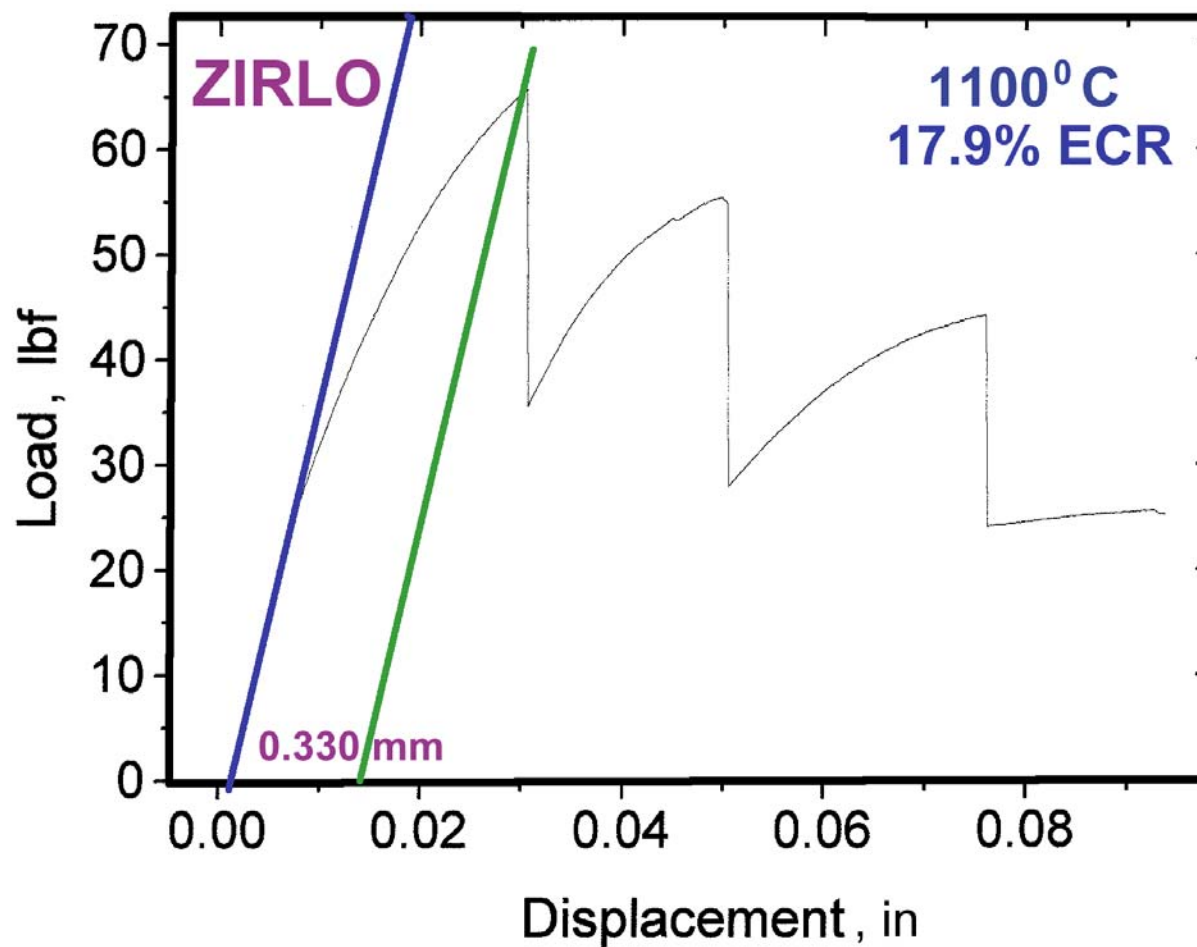


Fig. B.9 Ring-compression load-displacement data for ZIRLO oxidized to  $\approx 18\%$  ECR at  $1100^{\circ}\text{C}$ . Sample fractured into four pieces – only three were recovered after the test.

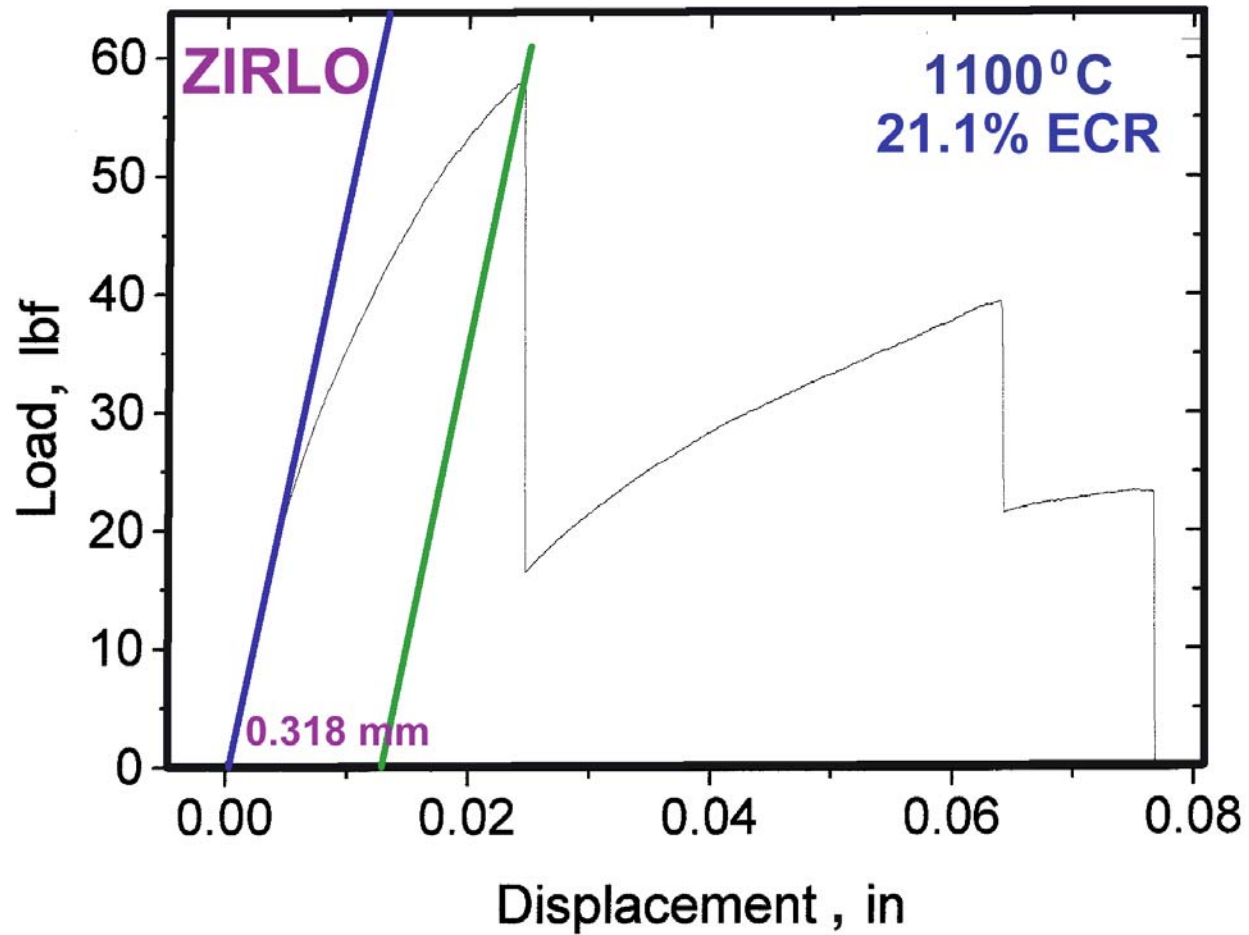


Fig. B.10 Ring-compression load-displacement data for ZIRLO oxidized to  $\approx 21\%$  ECR at  $1100^{\circ}\text{C}$ . Sample fractured into 4 pieces. The first load drop represents two through-wall failures.